Eur. Phys. J. C (2025) 85:1055
https://doi.org/10.1140/epjc/s10052-025-14774-x

THE EUROPEAN PHYSICAL JOURNAL C

Regular Article - Theoretical Physics

A comprehensive approach to the physics of mesons

A. S. Miramontes[1,a], **J. M. Morgado**[1,b], **J. Papavassiliou**[1,2,c], **J. M. Pawlowski**[2,3,d]

[1] Department of Theoretical Physics and IFIC, University of Valencia and CSIC, 46100 Valencia, Spain
[2] ExtreMe Matter Institute EMMI, GSI, Planckstrasse 1, 64291 Darmstadt, Germany
[3] Institut für Theoretische Physik, Universität Heidelberg, Philosophenweg 16, 69120 Heidelberg, Germany

Received: 30 July 2025 / Accepted: 9 September 2025

Abstract We develop an inclusive approach for the self-consistent solution of coupled sets of Bethe-Salpeter and Schwinger–Dyson equations in QCD. This framework allows us to maintain the axial Ward-Takahashi identities of the theory within advanced approximation schemes, such as the skeleton or three-particle irreducible expansions. For this purpose we reformulate the Schwinger-Dyson equation of the axial-vector vertex such that the bulk of its quantum corrections is expressed in terms of an effective vertex, containing an additional gluon. Crucially, this vertex satisfies a symmetry-induced relation of its own, which involves the full quark-gluon vertex. As a result, the Schwinger-Dyson equation reproduces the standard Ward-Takahashi identity satisfied by the axial-vector vertex. Consequently, the known relation between the quark mass function and the wave function of the pion in the chiral limit is duly fulfilled. The present approach offers valuable insights into the interplay between symmetry and dynamics, and provides a practical path towards computations of hadron physics within sophisticated approximations. In particular, the one-loop dressed truncation of the key dynamical equations, including that of the quark-gluon vertex, is shown to be completely compatible with the required symmetry relations. Further extensions and potential phenomenological applications of the developed framework are briefly discussed.

1 Introduction

In recent years, our quantitative understanding of the correlation functions of QCD has advanced considerably, mainly due to the ongoing efforts of functional approaches, such as Schwinger-Dyson equations (SDEs), for reviews see *e.g.*, [1–12], and the functional renormalization group (fRG), for QCD-related reviews see *e.g.*, [13–20]. In fact, by now, the results for quark-gluon correlation functions from functional approaches are in excellent agreement with that from gauge-fixed lattice simulations.

However, the incorporation of this extensive knowledge into the physics of hadrons is far from straightforward, chiefly due to incompatibilities between standard truncation schemes and the underlying fundamental symmetries, expressed through the Ward-Takahashi identities (WTIs). In fact, to date, most applications of functional approaches to hadronic physics are still based on the rainbow ladder (RL) approximation [21–34]; for works beyond RL, see, *e.g.*, [35–49]. This method and its variants [50–54] encompass a special type of QCD-derived information, typically amassed into propagator-like constructs (*e.g.*, effective charges [47,55–58]), but do not include the information encoded in the dressings of the fundamental QCD vertices, and in particular, of the quark-gluon vertex, Γ_μ.

In general, the physics of hadrons involves a large set of dynamical equations, non-trivially coupled to each other [1,3,8]. In particular, the standard SDEs for the quark-gluon correlation functions must be combined with the appropriate bound-state equations, namely the Bethe-Salpeter equations (BSEs) in the case of mesons [59,60], or the Faddeev equations in the case of baryons [61–70]. Focusing on mesons, in order for a self-consistent solution to emerge, any approximation implemented at the level of the SDEs must be appropriately incorporated into the BSEs. In fact, a pivotal consistency requirement of any truncation scheme is that the WTIs [71–75] be exactly preserved, in order for the chiral dynamics to be faithfully captured. The tension within the existing approaches may be summarized by stating that the proper treatment of the quark gap equation is known to require quite

[a] e-mail: angel.s.miramontes@uv.es
[b] e-mail: jose.m.morgado@uv.es
[c] e-mail: joannis.papavassiliou@uv.es (corresponding author)
[d] e-mail: j.pawlowski@thphys.uni-heidelberg.de

Published online: 24 September 2025

elaborate ingredients, whose incorporation into the BSEs destabilizes the WTIs. Therefore, it is highly desirable to set up functional approaches that allow for self-consistent computations, by including or computing state-of-the-art QCD correlation functions. This would allow us to use the respective quantitative functional results from *e.g.*, [39,49,76–99], as well as results from gauge-fixed lattice simulations, see *e.g.*, [100–121].

Given the key rôle played by the WTIs, in the present work we shall use chiral self-consistency as our main guiding principle. In particular, the main element we introduce is to enforce *exactly* the WTI satisfied by the flavour non-singlet axial-vector vertex, Γ^{μ}_5, at the level of the SDE that governs this vertex, employing the form first presented in [122,123] This is carried out first at the level of the complete SDE, and then within its "one-loop dressed" approximation. It turns out that the success of this endeavor hinges on the use of a quark-gluon vertex that contains nontrivial dressings for all of its form factors. In fact, quite importantly, these dressings cannot be arbitrary; instead, they must be determined *dynamically*, as solutions of a standard version of the SDE that controls the evolution of Γ_μ.

In the remainder of this section we briefly elucidate the sequence of ideas followed in this work, and highlight the main results. To that end, we employ a visual overview of the key components of this analysis, shown in the panels (a)–(f) of Fig. 1. In particular, we have

(a) the quark propagator, $S(p)$, and the SDE (gap equation) that determines its momentum dependence; a key ingredient of this equation is the fully-dressed quark-gluon vertex, Γ_μ, discussed in the next panel.
(b) the quark-gluon vertex, $\Gamma_\mu(q, r, -p)$, and the one-loop dressed version of the corresponding SDE, obtained within the formalism of the three-particle-irreducible (3PI) effective action, at the three-loop order [41,80,99].
(c) the non-singlet standard axial-vector vertex, $\Gamma^{\mu}_5(P, p_2, -p_1)$, and the exact closed form of the SDE that governs it. In the limit $P \to 0$, this SDE collapses to the BSE that describes the properties of the pion. The second diagram on the r.h.s. is the standard RL contribution (with $\Gamma_\mu \to \gamma_\mu$). The third diagram is composed by a vertex denoted by $G^{\mu\nu}_5$, first introduced in [124] under the name $\Lambda^{\mu\nu}_5$, which captures *all* remaining contributions (see next panel); we refer to it as the *"gluon-axial-vector vertex"*. Note that $G^{\mu\nu}_5$ contains a pole in P^2, whose residue is related to the quark-gluon vertex.
(d) the dynamical equation that determines the gluon-axial-vector vertex, $G^{\mu\nu}_5$, in the one-loop dressed approximation.
(e) the axial WTI satisfied by Γ^{μ}_5, denoted for brevity by $[\text{WTI}]_{\Gamma_5}$, which involves a special combination of the full inverse quark propagator.
(f) the axial WTI satisfied by the vertex $G^{\mu\nu}_5$, called $[\text{WTI}]_{G_5}$; it is akin to that of Γ^{μ}_5, but involves the full quark-gluon vertex, Γ_μ, instead of the inverse quark propagator. We emphasize that this WTI corresponds to relation stated in Eq. 6 of [124].

For the benefit of the reader, in Fig. 2 we summarize the correlation functions entering in our analysis. Note also that throughout this article we use conventions and Feynman rules written in Minkowski space, see *e.g.*, [6,74].

The first important result presented in this work is the demonstration that the $[\text{WTI}]_{\Gamma_5}$ holds true at the level of the *full* SDE that governs the vertex Γ^{μ}_5, see panel (c). Note that, crucially, the $[\text{WTI}]_{\Gamma_5}$ involves the quark propagator, whose self-energy contains the full Γ_μ, see panel (a). This demonstration becomes possible precisely because of the inclusion of the vertex $G^{\mu\nu}_5$, contained in the third graph on the r.h.s. of panel (c); in particular, $G^{\mu\nu}_5$ eliminates exactly a symmetry violating contribution stemming from the second graph. We emphasize that the proof hinges on the validity of $[\text{WTI}]_{G_5}$, shown in panel (f).

There is an important consequence of this result, which brings us one step closer to the BSE satisfied by the pion. In particular, it is well-known that the dynamical breaking of the chiral symmetry is encoded in the emergence of a nonvanishing mass function, $B(p^2)$, which appears on the r.h.s. of the $[\text{WTI}]_{\Gamma_5}$, panel (e). The only way to reconcile this feature is by allowing for a massless pole in Γ^{μ}_5, whose residue is essentially the pion wave function. In the limit $P \to 0$, the main component of the pion wave function satisfies a fundamental relation, connecting it directly to the quark component $B(p^2)$. As we show in this work, the BSE satisfied by this component, derived as the $P \to 0$ of the SDE governing Γ^{μ}_5, panel (c), reduces precisely to the dynamical equation obtained for $B(p^2)$ from the gap equation in (a), with Γ_μ fully-dressed. We stress that, at this point, Γ_μ is complete; in particular, it is *not* approximated by the SDE in panel (b), which has not yet been employed.

Since, for practical purposes, the SDE of Γ^{μ}_5 may not be treated exactly, it is of the utmost importance to implement a truncation that would respect an approximate version of the aforementioned key properties. This brings us to a key aspect of this work. In particular, the one-loop dressed version of $G^{\mu\nu}_5$ in panel (d) satisfies a very concrete version of the $[\text{WTI}]_{G_5}$ in panel (f): the Γ_μ that emerges on the r.h.s. of the $[\text{WTI}]_{G_5}$ *must* solve the one-loop dressed version of its own SDE, shown in panel (b)! Thus, the dynamics and symmetries captured by all panels of Fig. 1 are mutually compatible and coherently intertwined.

The article is organized as follows. In Sect. 2, we review certain key aspects of the quark propagator and the quark-gluon vertex, and discuss the form of the SDEs that govern their evolution. Next, in Sect. 3, we present the WTIs of the

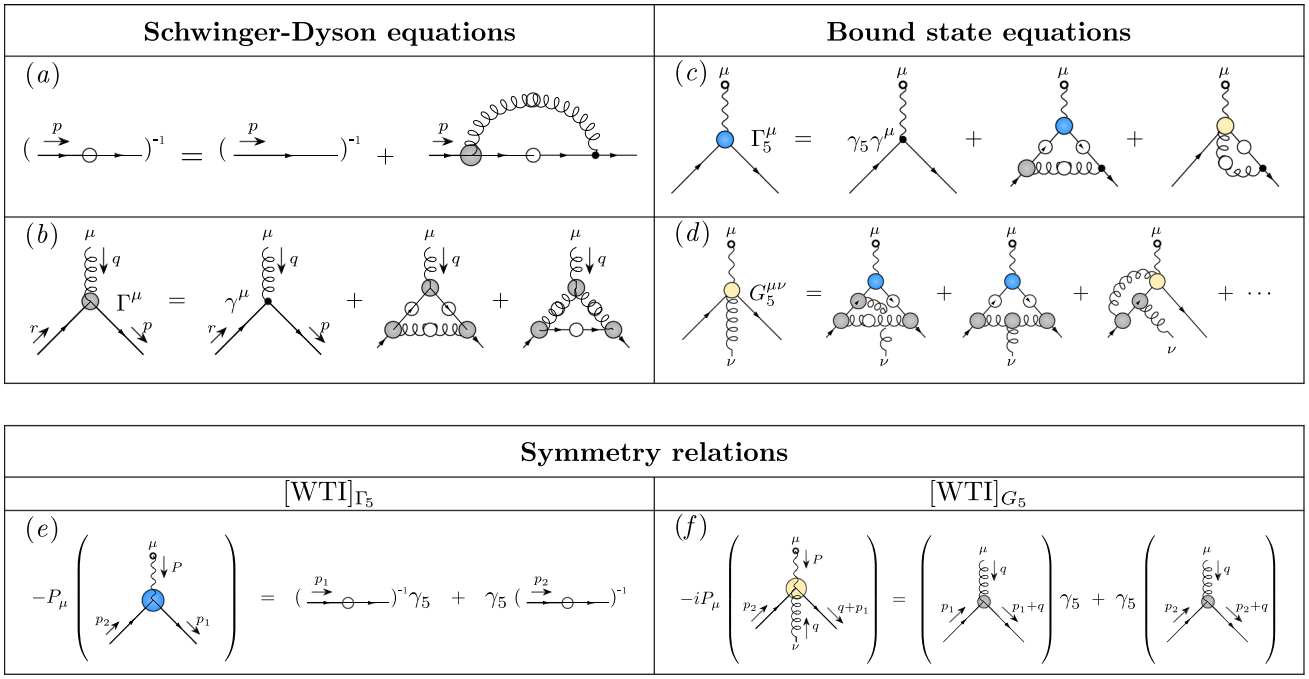

Fig. 1 Summary of the main building blocks of this work, shown graphically in panels (**a**)–(**f**): **a** quark gap equation; **b** one-loop dressed version of the quark-gluon vertex SDE; **c** axial-vector vertex SDE; **d** one-loop dressed version of the gluon-axial-vector vertex SDE; **e** axial-vector vertex WTI; and **f** gluon-axial-vector vertex WTI

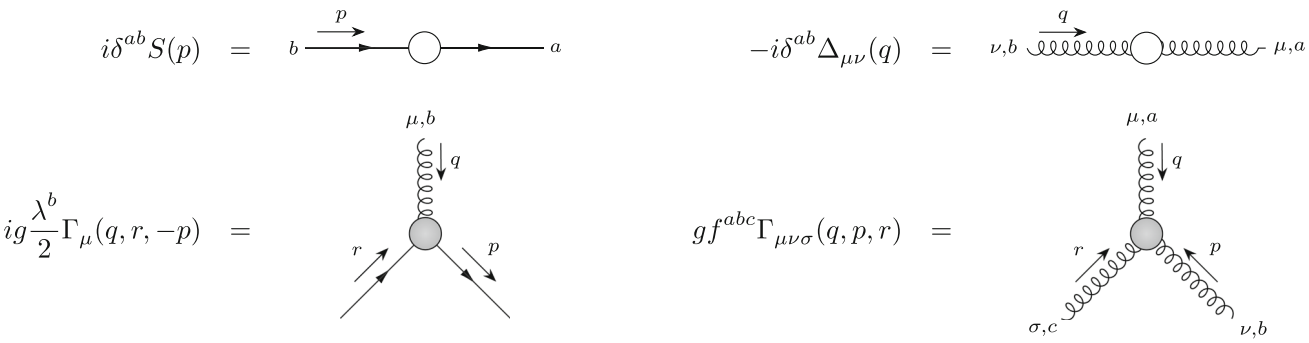

Fig. 2 Diagrammatic representation of the elementary Green functions appearing in this work: *top-left*: quark propagator; *top-right*: gluon propagator; *bottom-left*: quark-gluon vertex; and *bottom-right*: three-gluon vertex

two axial-vector vertices, Γ_5^μ and $G_5^{\mu\nu}$, and their respective pole contents, imposed by the dynamical breaking of the chiral symmetry. In Sect. 4 we demonstrate that the SDE of the Γ_5^μ reproduces the correct WTI, provided that the vertex $G_5^{\mu\nu}$ is properly included in the SDE kernel. In Sect. 5, we show that, in the chiral limit, the previous SDE reproduces exactly the fundamental relation between the pion Bethe-Salpeter Amplitude (BSA) and the quark mass function. In Sect. 6, we consider the one-loop dressed approximation of $G_5^{\mu\nu}$, and show that the WTI is exactly fulfilled provided that the quark-gluon vertex satisfies its own SDE, also approximated at the one-loop dressed level. Then, the self-consistent implementation of the above-mentioned approximations at the level of the SDE for Γ_5^μ is carried out in Sect. 7. In Sect. 8 we summarize our results and discuss possible future directions. Lastly, in App. A we demonstrate the WTIs obeyed by Γ_5^μ and $G_5^{\mu\nu}$, while in App. **??** we comment on the differences between flavour singlet and non-singlet axial-vector currents.

2 Quark propagator and quark-gluon vertex

In this section we review the main properties of two fundamental ingredients of our analysis, namely the quark propagator and the quark-gluon vertex.

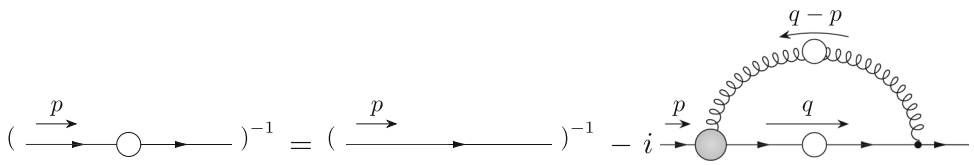

Fig. 3 Pictorial representation of the quark gap equation. The white circles denote full propagators, while the gray circle stands for the fully-dressed quark-gluon vertex, Γ_μ

The starting point of our considerations is the quark propagator, $S^{ab}(p)$, depicted in Fig. 2, which we cast in the standard form $S^{ab}(p) = i\delta^{ab}S(p)$, see *e.g.*, [74]. Typically, one decomposes the inverse quark propagator, $S^{-1}(p)$, as

$$S^{-1}(p) = A(p^2)p\!\!\!/ - B(p^2)\,, \tag{2.1}$$

where $A(p^2)$ and $B(p^2)$ are the dressings of the (Dirac) vector and scalar structures, respectively. The renormalization-group invariant (RGI) quark mass function, $\mathcal{M}(p^2)$, is given by $\mathcal{M}(p^2) = B(p^2)/A(p^2)$.

For the purposes of the present analysis, it is useful to also introduce the Dirac decomposition of $S(p)$, namely

$$S(p) = a(p^2)p\!\!\!/ + b(p^2), \tag{2.2}$$

with

$$a(p^2) = c(p^2)A(p^2), \qquad b(p^2) = c(p^2)B(p^2),$$
$$c(p^2) := \frac{1}{A^2(p^2)p^2 - B^2(p^2)}. \tag{2.3}$$

The momentum evolution of the functions $A(p^2)$ and $B(p^2)$ is determined from the SDE that governs the quark propagator, the *gap equation*,

$$S^{-1}(p) = p\!\!\!/ - m - i\Sigma(p), \tag{2.4}$$

and it is shown diagrammatically in Fig. 3. In Eq. (2.4), $\Sigma(p)$ stands for the quark self-energy,

$$\Sigma(p) = -g^2 C_f \int_q \gamma^\nu S(q)\Gamma^\mu(q-p,p,-q)\Delta_{\mu\nu}(q-p), \tag{2.5}$$

where g is the QCD gauge coupling and $C_f = 4/3$ the Casimir eigenvalue of the fundamental SU(3) representation. In addition, the integral measure is denoted by

$$\int_q := \int_{R^4} \frac{\mathrm{d}^4 q}{(2\pi)^4}, \tag{2.6}$$

where the use of a symmetry-preserving regularization scheme is implicitly assumed. Moreover, $\Delta_{\mu\nu}$ and Γ_μ represent the full gluon propagator and the fully-dressed quark-gluon vertex, respectively, to be discussed below. Finally, m stands for the current quark mass; note that, throughout this work, we restrict ourselves to the case $m = 0$ (chiral limit).

In the covariant (R_ξ) gauges [125], the gluon propagator, $\Delta^{ab}_{\mu\nu}(q) = -i\delta^{ab}\Delta_{\mu\nu}(q)$, assumes the general form

$$\Delta_{\mu\nu}(q) = \Delta(q^2)\,P_{\mu\nu}(q) + \xi\frac{q_\mu q_\nu}{q^4}, \tag{2.7}$$

where $P_{\mu\nu}(q) = g_{\mu\nu} - q_\mu q_\nu/q^2$ is the transverse projection operator and ξ is the gauge-fixing parameter; for the diagrammatic representation of the gluon propagator see Fig. 2. The function $\Delta(q^2)$ denotes the scalar component of the gluon propagator and depends explicitly on ξ. Note that in practical applications one uses almost exclusively the Landau gauge ($\xi = 0$), which brings about certain simplifications in the treatment of the gap equation. However, in the present analysis we will keep a general value of ξ, since, as we will see, none of the ensuing demonstrations depends on the gauge choice.

The quark-gluon vertex (see Fig. 2) is defined as $\Gamma^b_\mu(q,r,-p) = ig\frac{\lambda^b}{2}\Gamma_\mu(q,r,-p)$, with λ^b denoting the standard Gell-Mann matrices ($b = 1,\ldots,8$). The part $\Gamma^\mu(q,r,-p)$ is typically decomposed in a tensorial basis composed by 12 elements, to be denoted by $\tau^\mu_i(q,r,-p)$; for some standard choices of bases in the literature, see, *e.g.*, [84,126–128]. Thus,

$$\Gamma^\mu(q,r,-p) = \sum_{i=1}^{12}\lambda_i(q,r,-p)\tau^\mu_i(q,r,-p), \tag{2.8}$$

where the scalar functions $\lambda_i(q,r,-p)$ are the associated form factors or dressings. Note that, in the Landau gauge ($\xi = 0$), the number of basis elements is reduced to eight, and the vertex is usually referred to as the "transversely projected" vertex, see, *e.g.*, [97], and references therein.

In what follows we will make extensive use of the separation of Γ^μ into two components, Γ^μ_1 and Γ^μ_2, comprised by the basis elements τ^μ_i that contain an odd or even number of Dirac γ matrices, respectively. In particular, we may enumerate the basis elements τ^μ_i such that the first (last) six contain an odd (even) number of Dirac γ matrices, and define

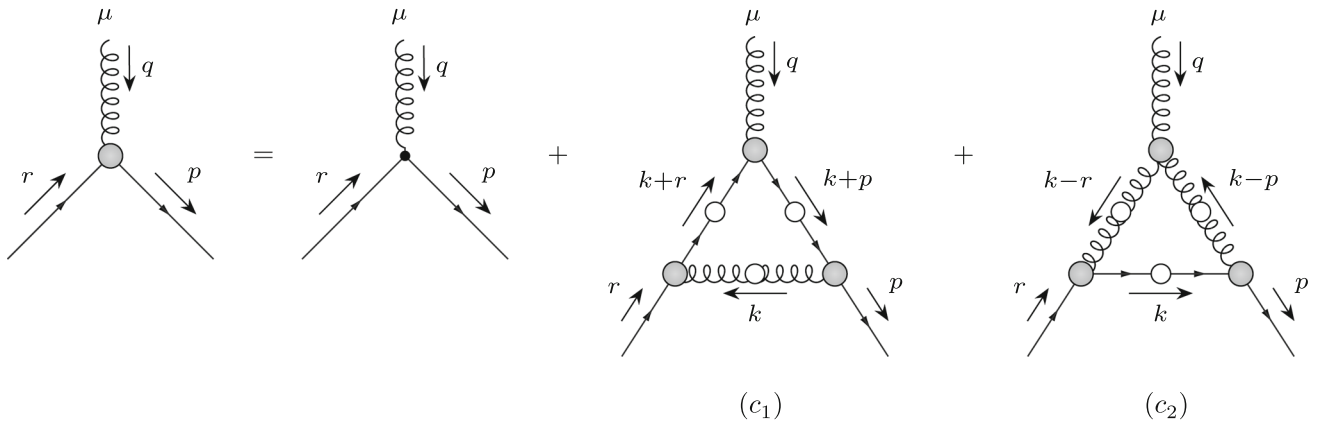

Fig. 4 Diagrammatic representation of the full quark-gluon vertex SDE, obtained from a three-loop truncation of the 3PI effective action. Gray circles represent the fully-dressed quark-gluon and three-gluon vertices, while white ones identify full quark and gluon propagators. Diagrams (c_1^μ) and (c_2^μ) are often referred to as "abelian" and "non-abelian", respectively

$$\Gamma_1^\mu(q,r,-p) := \sum_{i=1}^{6} \lambda_i(q,r,-p)\tau_i^\mu(q,r,-p),$$
$$\Gamma_2^\mu(q,r,-p) := \sum_{i=7}^{12} \lambda_i(q,r,-p)\tau_i^\mu(q,r,-p), \tag{2.9}$$

such that

$$\Gamma^\mu(q,r,-p) = \underbrace{\Gamma_1^\mu(q,r,-p)}_{\text{odd \# of } \gamma} + \underbrace{\Gamma_2^\mu(q,r,-p)}_{\text{even \# of } \gamma}. \tag{2.10}$$

For a given basis, the above decomposition is unique. As it will become clear in what follows, the decomposition in Eq. (2.10) appears naturally in various points of the subsequent analysis, where we will take advantage of the elementary relations

$$\mathrm{Tr}\big[(\text{even \# of } \gamma)\times\Gamma_1^\mu\big] = 0 = \mathrm{Tr}\big[(\text{odd \# of } \gamma)\times\Gamma_2^\mu\big], \tag{2.11}$$

and, in addition,

$$\gamma_5\Gamma^\mu = \gamma_5(\Gamma_1^\mu + \Gamma_2^\mu) = (\Gamma_2^\mu - \Gamma_1^\mu)\gamma_5. \tag{2.12}$$

In principle, the evolution of the form factors λ_i is determined from the full SDE satisfied by $\Gamma_\mu(q,r,-p)$. To be sure, in practice one employs truncated versions of the SDE, thus obtaining approximate results for the λ_i. One of the standard approximations of the SDE, extensively employed in the recent literature, is shown in Fig. 4; this particular SDE is obtained from the 3PI effective action at the three-loop order [41,80,129–132]. One of the special characteristics of the SDE in Fig. 4 is that all fundamental vertices inside the diagrams (c_1^μ) and (c_2^μ) are fully dressed. This is to be contrasted with the standard SDE formulation (see *e.g.*, [80] and references therein), where one of the vertices is always kept at its classical (tree-level) form. Note that, equivalently, one may reach the form of the SDE in Fig. 4 by resorting to the standard skeleton expansion [47].

The dynamical equation depicted in Fig. 4 represents a typical case of an SDE truncated at the *"one-loop dressed"* level: it is comprised by the pair of one-loop diagrams known from perturbation theory, but with all propagators and vertices fully dressed. Given that this particular version of the SDE plays a crucial rôle in the construction presented in Sect. 6, we find it useful to denote the corresponding solution by $\Gamma_\mu^{(1)}$, namely

$$\Gamma_\mu^{(1)} = \gamma_\mu + (c_{1\mu}) + (c_{2\mu}), \tag{2.13}$$

with the two loop parts c_1 and c_2. They read

$$\begin{aligned}(c_{1\mu}) = c_a \int_k \Gamma_\beta^{(1)}(-k,k+p,-p)S(k+p)\\ \Gamma_\mu^{(1)}(q,k+r,-k-p)S(k+r)\Gamma_\alpha^{(1)}\\ \times(k,r,-k-r)\Delta^{\alpha\beta}(k),\end{aligned} \tag{2.14}$$

and

$$\begin{aligned}(c_{2\mu}) = c_b \int_k \Gamma_\beta^{(1)}(p-k,k,-p)S(k)\Gamma_\alpha^{(1)}(k-r,r,-k)\\ \Gamma_{\mu\rho\sigma}(q,k-p,k-r)\times\Delta^{\rho\beta}(k-p)\Delta^{\alpha\sigma}(k-r),\end{aligned} \tag{2.15}$$

where $\Gamma_{\mu\rho\sigma}$ is the full three-gluon vertex shown in Fig. 2 and with the prefactors

$$c_a := -ig^2\left(C_f - \frac{C_A}{2}\right), \quad c_b := ig^2\frac{C_A}{2}. \tag{2.16}$$

We emphasize once again that Γ_μ is the exact quark-gluon vertex, while $\Gamma^{(1)}_\mu$ is an approximation to it, obtained from a truncated SDE. Thus, in general, $\Gamma_\mu \neq \Gamma^{(1)}_\mu$, even though the differences are expected to be small. The distinction between Γ_μ and $\Gamma^{(1)}_\mu$ will be maintained in what follows; thus, the exact results presented in Secs. 3, 4, and 5 involve the former, while the one-loop dressed construction of Sect. 6 entails the latter.

Returning to the quark gap equation of Eq. (2.4), we may suitably project out the coupled system that determines $A(p^2)$ and $B(p^2)$; specifically, taking the trace of Eq. (2.4) isolates the equation for $B(p^2)$, while multiplying by $p\!\!/$ and then taking the trace selects $A(p^2)$. Thus, we obtain

$$\begin{aligned} p^2A(p^2) = p^2 &+ \frac{ig^2C_f}{4}\int_q a(q^2)\mathrm{Tr} \\ &\left[p\!\!/\gamma^\nu q\!\!/\,\Gamma^\mu_1(q-p,p,-q)\right]\Delta_{\mu\nu}(q-p) \\ &+\frac{ig^2C_f}{4}\int_q b(q^2)\mathrm{Tr} \\ &\left[p\!\!/\gamma^\nu\Gamma^\mu_2(q-p,p,-q)\right]\Delta_{\mu\nu}(q-p), \end{aligned} \tag{2.17}$$

and

$$\begin{aligned} B(p^2) = -&\frac{ig^2C_f}{4}\int_q a(q^2)\mathrm{Tr} \\ &\left[\gamma^\nu q\!\!/\,\Gamma^\mu_2(q-p,p,-q)\right]\Delta_{\mu\nu}(q-p) \\ -&\frac{ig^2C_f}{4}\int_q b(q^2)\mathrm{Tr} \\ &\left[\gamma^\nu\Gamma^\mu_1(q-p,p,-q)\right]\Delta_{\mu\nu}(q-p), \end{aligned} \tag{2.18}$$

where we note in both Eqs. (2.17) and (2.18) the appearance of the components Γ^μ_1 and Γ^μ_2, introduced in Eq. (2.10).

Observe finally that in the RL approximation, where $\Gamma_\mu \to \gamma_\mu$ (and $\xi = 0$), the quark self-energy of Eq. (2.5) becomes

$$\Sigma_{\rm RL}(p) = -g^2C_f\int_q \gamma^\nu S(q)\gamma^\mu\Delta_{\mu\nu}(q-p), \tag{2.19}$$

and the system of Eqs. (2.17) and (2.18) collapses to

$$\begin{aligned} p^2A(p^2) &= p^2 + \frac{ig^2C_f}{4}\int_q a(q^2)\mathrm{Tr}\left[p\!\!/\gamma^\nu q\!\!/\gamma^\mu\right]\Delta_{\mu\nu}(q-p), \\ B(p^2) &= -\frac{ig^2C_f}{4}\int_q b(q^2)\mathrm{Tr}\left[\gamma^\nu\gamma^\mu\right]\Delta_{\mu\nu}(q-p). \end{aligned} \tag{2.20}$$

3 Axial vertices and their Ward–Takahashi identities

When contracted by P_μ, the axial vertices $\Gamma^\mu_5(P,p_2,-p_1)$ and $G^{\mu\nu}_5(P,p_2,q,-p_1-q)$, shown in Fig. 5, satisfy abelian WTIs, denoted by $[\mathrm{WTI}]_{\Gamma_5}$ and $[\mathrm{WTI}]_{G_5}$, respectively. While the former is well-known, see, *e.g.*, [73,75], the latter has received little attention [122–124]. In this section we discuss these WTIs, and the constraints they impose on the pole structure of the two axial vertices.

3.1 Axial-vector vertex Γ^μ_5

Consider the flavour non-singlet axial-vector vertex Γ^μ_5 (Fig. 5), defined as the amputated part of the correlation function $\langle 0|Tj^\mu_5(y)\psi(x_1)\bar\psi(x_2)|0\rangle$ (see App. A). The (non-singlet) axial-vector current is given by $j^\mu_5(x) = \bar\psi(x)\gamma_5\gamma^\mu t^a\psi(x)$, where the t^a are the flavour $SU(N_f)$ generators which, for the shortness, we are systematically dropping.

In momentum space, and in the absence of current quark masses ($m = 0$), the vertex $\Gamma^\mu_5(P,p_2,-p_1)$ satisfies the axial WTI [73–75] (see App. A for the derivation)

$$\begin{aligned} [\mathrm{WTI}]_{\Gamma_5} \;:\; &-P_\mu\Gamma^\mu_5(P,p_2,-p_1) \\ &= S^{-1}(p_1)\gamma_5 + \gamma_5 S^{-1}(p_2). \end{aligned} \tag{3.1}$$

In the limit $P \to 0$, in which case $p_1 = p_2 := p$, this identity reveals a profound connection between the term $B(p^2)$, which emerges when the chiral symmetry is dynamically broken, and the amplitude that controls the formation of a pion as a quark-antiquark bound state.

In particular, it is well-known that, in the presence of a non-vanishing $B(p^2)$, the only way to satisfy Eq. (3.1) is to allow $\Gamma^\mu_5(P,p_2,-p_1)$ to exhibit a pole at $P^2 = 0$, which is associated with the corresponding massless Goldstone boson, *i.e.*, the pion.

Specifically, if we substitute the decomposition of Eq. (2.1) into Eq. (3.1) and implement the limit $P \to 0$, the terms proportional to $A(p^2)$ drop out, and we find

$$\lim_{P\to 0} P_\mu\Gamma^\mu_5(P,p_2,-p_1) = 2B(p^2)\gamma_5. \tag{3.2}$$

This observation leads us to conclude that Γ^μ_5 must display a pole in P^2, *i.e.*,

$$\begin{aligned} \Gamma^\mu_5(P,p_2,-p_1) = \Gamma^\mu_5(P,p_2,-p_1)\big|_{\rm pole} \\ + \Gamma^\mu_5(P,p_2,-p_1)\big|_{\rm reg}\,, \end{aligned} \tag{3.3}$$

with

$$\Gamma^\mu_5(P,p_2,-p_1)\big|_{\rm pole} = \frac{P^\mu}{P^2}\,\chi(P,p_2,-p_1)\gamma_5\,, \tag{3.4}$$

where $\chi(P,p_2,-p_1)$ is the BSA of the pion. Note that we suppress the pion decay constant, f_π, which is typically introduced at this point, see, *e.g.*, [75,133].

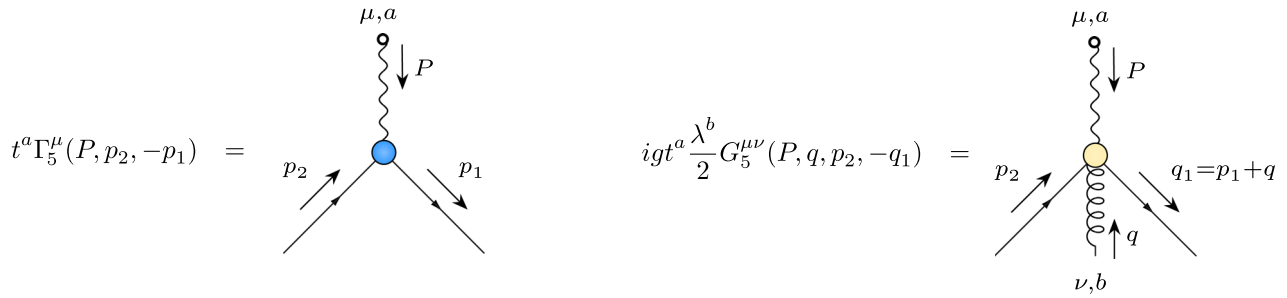

Fig. 5 Diagrammatic representation of the two central vertices treated in this work: *left-panel*: axial-vector vertex; *right-panel*: gluon-axial-vector vertex

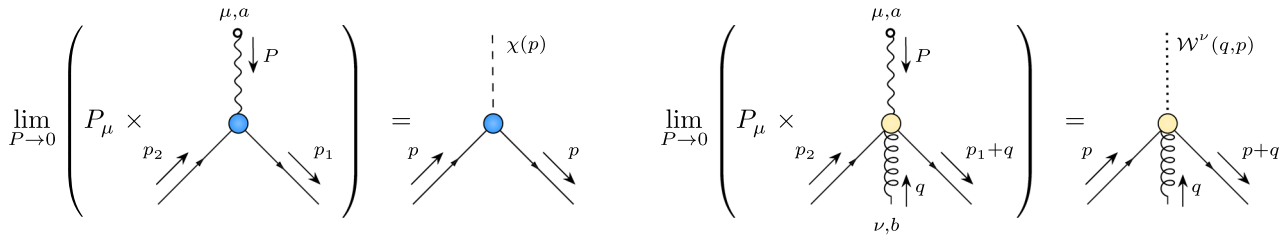

Fig. 6 Diagrammatic representation of the pole contributions to the two axial vertices under consideration: *left-panel*: pole residue of the axial-vector vertex; *right-panel*: pole residue of the gluon-axial-vector vertex

Using Eq. (3.3), it is straightforward to show that, in the limit $P \to 0$,

$$\lim_{P\to 0} P_\mu\Gamma_5^\mu(P,\,p_2,-p_1) = \lim_{P\to 0} P_\mu\Gamma_5^\mu(P,\,p_2,-p_1)\big|_{\text{pole}} = \chi(0,\,p,-p)\gamma_5. \tag{3.5}$$

a result whose diagrammatic representation is shown in the left-panel of Fig. 6. Then, combining Eqs. (3.2) and (3.5), we find

$$\chi(0,\,p,-p) = 2B(p^2), \tag{3.6}$$

where the γ_5 has been canceled from both sides.

The relation in Eq. (3.6) may be further inspected, by resorting to the standard tensorial decomposition for the amplitude $\chi(P,\,p_2,-p_1)$ [75]

$$\chi(P,\,p_2,-p_1) = \chi_1 + \chi_2 p\!\!\!/ + \frac{1}{2}\chi_3(p\!\!\!/_1 + p\!\!\!/_2) + i\chi_4[p\!\!\!/_1,\,p\!\!\!/_2]\,, \tag{3.7}$$

where the $\chi_i = \chi_i(P,\,p_2,-p_1)$ are the associated form factors, which depend on three Lorentz scalars (*e.g.*, p_1^2, p_2^2 and $p_1\cdot p_2$). In particular, when $P \to 0$, we have

$$\chi(0,\,p,-p) = \chi_1(p^2) + \chi_3(p^2)p\!\!\!/. \tag{3.8}$$

Then, from Eq. (3.6) we obtain the two basic relations [38, 133],

$$\chi_1(p^2) = 2B(p^2), \tag{3.9}$$

and

$$\chi_3(p^2) = 0. \tag{3.10}$$

Notably, Eq. (3.10) may also be directly derived from the tensor decomposition in Eq. (3.7), as a consequence of charge conjugation invariance.

3.2 Gluon-axial-vector vertex $G_5^{\mu\nu}$

The second main element of our construction is the gluon-axial-vector vertex, $G_5^{\mu\nu}$ (Fig. 5). This particular vertex is defined as the amputated and 1PI part of the correlation function comprised by a quark-antiquark pair, a gluon field, and an axial-vector current j_5^μ, App. A.2.

In the absence of current quark masses, $G_5^{\mu\nu}(P,\,q,\,p_2,\,-q_1)$ satisfies the axial WTI (see App. A for the derivation and [9,122–124] for additional discussions.)

$$[\text{WTI}]_{G_5}\;:\quad -iP_\mu G_5^{\mu\nu}(P,\,q,\,p_2,\,-q_1) = \Gamma^\nu(q,\,p_1,\,-q_1)\gamma_5 + \gamma_5\Gamma^\nu(q,\,p_2,\,-q_2), \tag{3.11}$$

where $q_i := p_i + q$. Note that, since $\gamma^\nu\gamma_5 + \gamma_5\gamma^\nu = 0$, the combination of vertices appearing on the r.h.s. of Eq. (3.11) does not contain tree-level contributions, *i.e.*,

$$-iP_\mu G_5^{\mu\nu}(P,\,q,\,p_2,\,-q_1) = \Gamma_Q^\nu(q,\,p_1,\,-q_1)\gamma_5 + \gamma_5\Gamma_Q^\nu(q,\,p_2,\,-q_2), \tag{3.12}$$

where

$$\Gamma^{\nu}_{Q}(q,r,-p) := \Gamma^{\nu}(q,r,-p) - \lambda_1(q,r,-p)\gamma^{\nu}. \tag{3.13}$$

This observation is consistent with the fact that the vertex $G_5^{\mu\nu}$, appearing on the l.h.s. of Eq. (3.12), does not possess a tree-level term.

As in the case of the axial-vector vertex, this WTI imposes strong constraints on $G_5^{\mu\nu}$. Similarly to the previous case, Eq. (3.11) requires the gluon-axial-vector vertex to have a longitudinally coupled pole. In fact, taking the limit $P \to 0$ of this identity, the terms involving Γ_1^{ν} drop out, and we are left with

$$\begin{aligned}\lim_{P\to 0} P_\mu G_5^{\mu\nu}(P,q,p_2,-q_1) &= i\left[\Gamma^{\nu}(q,p,-p-q)\gamma_5 + \gamma_5\Gamma^{\nu}(q,p,-p-q)\right]\\ &= 2i\Gamma_2^{\nu}(q,p,-p-q)\gamma_5,\end{aligned} \tag{3.14}$$

where $\Gamma_2^{\nu}(q,p,-p-q)$ is the even part of the quark-gluon vertex $\Gamma^{\nu}(q,p,-p-q)$. Note that $\Gamma^{\nu}(q,p,-p-q)$ corresponds to the quark-gluon vertex shown in Fig. 4, but with $r \leftrightarrow p$.

We emphasize that, crucially, Γ_2^{ν} is comprised precisely by the terms referred to as *chiral symmetry breaking* components (see, *e.g.*, [97,99]): when solving the SDE of the quark-gluon vertex, they arise only when a nontrivial $B(p^2)$ has emerged from the quark gap equation. Thus, it is precisely the part of the quark-gluon vertex induced by the breaking of chiral symmetry that saturates the pole residue of $G_5^{\mu\nu}$.

To explore this point in some detail, we note that, in complete analogy to Γ_5^{μ}, Eq. (3.14) can be resolved only if $G_5^{\mu\nu}$ possesses a pole in $P^2 = 0$, *i.e.*,

$$\begin{aligned}G_5^{\mu\nu}(P,q,p_2,-q_1) = G_5^{\mu\nu}(P,q,p_2,-q_1)\big|_{\text{pole}}\\ + G_5^{\mu\nu}(P,q,p_2,-q_1)\big|_{\text{reg}},\end{aligned} \tag{3.15}$$

with

$$G_5^{\mu\nu}(P,q,p_2,-q_1)\big|_{\text{pole}} = 2i\,\frac{P^{\mu}}{P^2}\,\mathcal{W}^{\nu}(P,q,p_2,-q_1)\gamma_5. \tag{3.16}$$

At the formal level, the component $\mathcal{W}^{\nu}$ plays a rôle analogous to that of the amplitude χ in Eq. (3.4), acting as a momentum-dependent residue. From the physical point of view, $\mathcal{W}^{\nu}$ encapsulates key pieces of the pion dynamics, contained in the SDE of the axial-vector vertex. In that sense, it may be viewed as a concise representation of various contributions that participate in the momentum evolution of the pion amplitude χ.

Using the decomposition of Eq. (3.15) in conjunction with Eq. (3.16), it is straightforward to show that (Fig. 6, right-panel)

$$\begin{aligned}&\lim_{P\to 0} P_\mu G_5^{\mu\nu}(P,q,p_2,-q_1)\\ &= \lim_{P\to 0} P_\mu\, G_5^{\mu\nu}(P,q,p_2,-q_1)\big|_{\text{pole}}\\ &= 2i\,\mathcal{W}^{\nu}(0,q,p,-p-q)\gamma_5 = 2i\,\Gamma_2^{\nu}(q,p,-p-q)\gamma_5,\end{aligned} \tag{3.17}$$

where, once again, $\Gamma_2^{\nu}(q,p,-p-q)$ is the even part of the quark-gluon vertex $\Gamma^{\nu}(q,p,-p-q)$.

It is clear that $\mathcal{W}^{\nu}(0,q,p,-p-q)$ admits the same tensorial decomposition as the quark-gluon vertex $\Gamma^{\nu}(q,r,-r-q)$ in Eq. (2.8), with the change $r \leftrightarrow p$, namely

$$\mathcal{W}^{\nu}(0,q,p,-p-q) = \sum_{i=1}^{12} w_i(q,p,-p-q)\tau_i^{\nu}(q,p,-p-q), \tag{3.18}$$

where the $w_i(q,p,-p-q)$ are the corresponding form factors (dressings). Evidently, as in Eq. (2.10), a separation into odd and even structures may be carried out (suppressing momenta)

$$\mathcal{W}^{\nu} = \mathcal{W}_1^{\nu} + \mathcal{W}_2^{\nu}, \tag{3.19}$$

with

$$\mathcal{W}_1^{\nu} = \sum_{i=1}^{6} w_i\tau_i^{\nu}, \qquad \mathcal{W}_2^{\nu} = \sum_{i=7}^{12} w_i\tau_i^{\nu}. \tag{3.20}$$

The substitution of the above tensor decomposition into Eq. (3.17) leads directly to the relations

$$\mathcal{W}_2^{\nu} = \Gamma_2^{\nu}(q,p,-p-q), \qquad \mathcal{W}_1^{\nu} = 0, \tag{3.21}$$

or, equivalently, at the level of the form factors

$$w_i(q,p,-p-q) = \lambda_i(q,p,-p-q), \qquad i = 7,\ldots,12, \tag{3.22}$$

and

$$w_i(q,p,-p-q) = 0, \qquad i = 1,\ldots,6\,; \tag{3.23}$$

which represent the direct analogues of Eqs. (3.9) and (3.10), respectively.

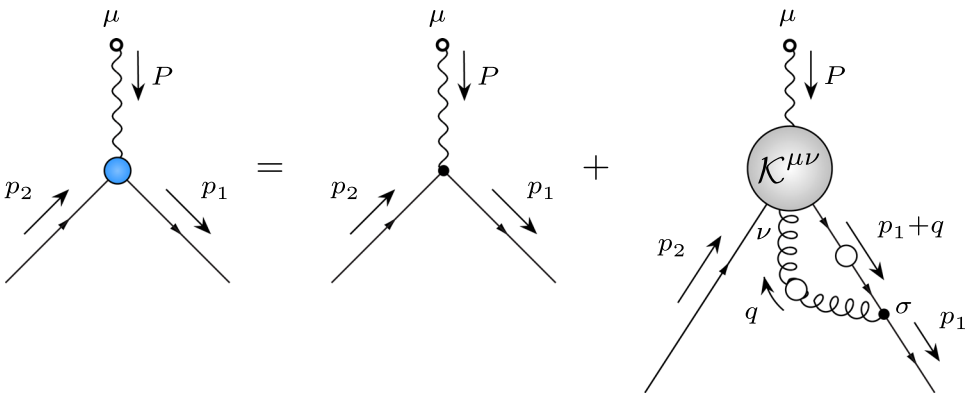

Fig. 7 Diagrammatic representation of the SDE satisfied by the axial-vector vertex Γ_5^μ, formulated from the point of view of the antiquark leg

4 The axial WTI from the vertex SDE: exact derivation

In this section we demonstrate that the exact dynamical equation (SDE) that governs the evolution of Γ_5^μ satisfies precisely the $[\text{WTI}]_{\Gamma_5}$ of Eq. (3.1).

To that end, instead of considering the SDE satisfied by Γ_5^μ from the perspective of the axial-vector current (leg with momentum P), we adopt the view of the antiquark leg, carrying momentum p_1; the resulting SDE is shown in Fig. 7. According to the standard rules, the vertex connecting the special leg to the rest of the diagram must be kept at tree-level (γ^σ in Fig. 7). This particular way of writing the SDE, *i.e.*, using an antifermion as the reference leg has been used in the studies of the ghost-gluon [4,134,135] and quark-gluon vertices [43].

Thus, the resulting SDE reads

$$\Gamma_5^\mu(P,p_2,-p_1) = \gamma_5\gamma^\mu + ig^2C_f\int_q \gamma^\sigma S(q_1)\mathcal{K}^{\mu\nu} \times (P,q,p_2,-q_1)\Delta_{\nu\sigma}(q), \tag{4.1}$$

where we have defined $q_1 := p_1 + q$. The kernel $\mathcal{K}^{\mu\nu}$ is comprised by four incoming operators, a quark (ψ), an antiquark ($\bar\psi$), a gluon (A^ν), and a axial-vector current (j_5^μ), so that $\mathcal{K}^{\mu\nu} := \mathcal{K}_{j_5^\mu A^\nu\psi\bar\psi}$. This kernel may be decomposed as shown in Fig. 8, namely

$$\mathcal{K}^{\mu\nu}(P,q,p_2,-q_1) = -\Gamma_5^\mu(P,q_2,-q_1)S(q_2) \Gamma^\nu(q,p_2,-q_2) + iG_5^{\mu\nu}(P,q,p_2,-q_1), \tag{4.2}$$

with $q_2 := p_2 + q$, and $G_5^{\mu\nu}$ is the gluon-axial-vector vertex introduced in Sect. 3.2.

As a result, the SDE of Γ_5^μ can be written as

$$\Gamma_5^\mu = \gamma_5\gamma^\mu + (a_5^\mu) + (b_5^\mu), \tag{4.3}$$

where

$$(a_5^\mu) = -ig^2C_f\int_q \gamma^\sigma S(q_1)\Gamma_5^\mu(P,q_2,-q_1)S(q_2) \Gamma^\nu(q,p_2,-q_2)\Delta_{\nu\sigma}(q)\,, \tag{4.4}$$

$$(b_5^\mu) = -g^2C_f\int_q \gamma^\sigma S(q_1)G_5^{\mu\nu}(P,q,p_2,-q_1)\Delta_{\nu\sigma}(q). \tag{4.5}$$

Note that the lowest-order diagram contributing to $\mathcal{K}^{\mu\nu}$ is enclosed in the blue-dashed box of (a_5^μ) in Fig. 8. A "cut" through the quark propagator with momentum p_2+q shows that this diagram is clearly one-particle reducible (1PR); of course, the full diagram, (a_5^μ), where the kernel is embedded, is one-particle irreducible (1PI). All remaining graphs contained in $\mathcal{K}^{\mu\nu}$ are 1PI, and coincide exactly with the graphs forming the vertex $G_5^{\mu\nu}$, which is enclosed entirely within the blue-dashed box in graph (b_5^μ).

If, instead, a flavour singlet axial-vector current is considered, a third diagrammatic contribution is present in the decomposition of $\mathcal{K}$, coupling the axial-vector current to a pair of gluons, see *e.g.*, [9] and references therein. However, as explained in App. **??**, this additional term vanishes in the non-singlet case, while in the singlet case contributes solely to the anomaly. In that sense, as long as the SDE of Eq. (4.3) describes the flavour non-singlet vertex, it is exact.

Given that the graphs (a_5^μ) and (b_5^μ) account for the full sum of all quantum corrections, if we contract both sides of Eq. (4.3) by P_μ,

$$P_\mu\Gamma_5^\mu(P,p_2,-p_1) = -(\not p_1\gamma_5+\gamma_5\not p_2) + P_\mu\left[(a_5^\mu)+(b_5^\mu)\right], \tag{4.6}$$

the r.h.s. of the $[\text{WTI}]_{\Gamma_5}$ in Eq. (3.1) must emerge exactly.

Let us focus on the contraction of graph (a_5^μ), which is the only loop contribution typically considered within the RL approximation. Using the r.h.s of Eq. (3.1) for the term $P_\mu\Gamma_5^\mu(P,q_2,-q_1)$ under the integral sign, we find

$$P_\mu(a_5^\mu) = ig^2C_f\int_q \gamma^\sigma S(q_1)\left[S^{-1}(q_1)\gamma_5+\gamma_5S^{-1}(q_2)\right] S(q_2)\Gamma^\nu(q,p_2,-q_2)\Delta_{\nu\sigma}(q)$$

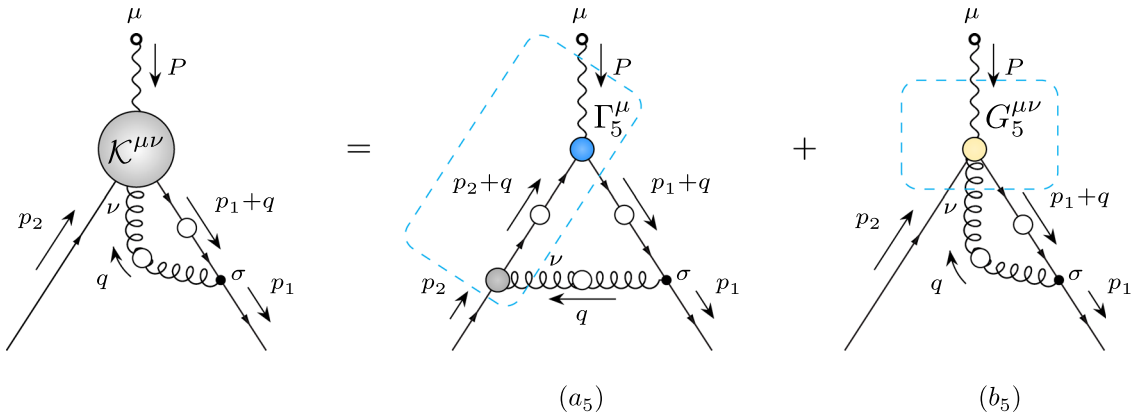

Fig. 8 Diagrammatic representation of the quantum part of the SDE in Fig. 7. The decomposition of $\mathcal{K}^{\mu\nu}$ given in Eq. (4.2) is delimited by the two blue-dashed boxes

$$= \gamma_5 \underbrace{\left[-ig^2 C_f \int_q \gamma^\sigma S(q_2)\Gamma^\nu(q, p_2, -q_2)\Delta_{\nu\sigma}(q)\right]}_{i\Sigma(p_2)} + \underbrace{ig^2 C_f \int_q \gamma^\sigma S(q_1)\gamma_5\Gamma^\nu(q, p_2, -q_2)\Delta_{\nu\sigma}(q)}_{V(p_1,p_2)\text{: symmetry violating term}}. \tag{4.7}$$

The result in Eq. (4.7) prompts the following observations:

(i) When the term $i\Sigma(p_2)$ of Eq. (4.7) is added to the term $-\gamma_5 \not{p}_2$ of Eq. (4.6), and after use of the gap equation in Eq. (2.4), one recovers precisely the term $-\gamma_5 S^{-1}(p_2)$ in $[\text{WTI}]_{\Gamma_5}$. However, the second term, $V(p_1, p_2)$, does not admit an interpretation as a genuine quark self-energy, leading to the obvious violation of the fundamental $[\text{WTI}]_{\Gamma_5}$.

(ii) Within the RL approximation, where $\Gamma_\nu(q, r, -p) \to \gamma_\nu$, the symmetry violating term $V(p_1, p_2)$ reduces to the required self-energy, since

$$V(p_1, p_2) \xrightarrow{\text{RL}} ig^2 C_f \int_q \gamma^\sigma S(q_1)\gamma_5\gamma^\nu \Delta_{\nu\sigma}(q) = i\Sigma_{\text{RL}}(p_1)\gamma_5. \tag{4.8}$$

Thus, diagram (a_5^μ) reproduces the $[\text{WTI}]_{\Gamma_5}$ in the RL approximation, but fails to do so when the full kinematic structure of the quark-gluon vertex is maintained.

(iii) One may recast the term $V(p_1, p_2)$ as the difference between the required quark self-energy, $i\Sigma(p_1)$, and a symmetry violating remainder, to be denoted by $\mathcal{V}(p_1, p_2)$, through the addition and subtraction of the term $\Gamma^\nu(q, p_1, -q_1)\gamma_5$, *i.e.*,

$$V(p_1, p_2) = \underbrace{\left[-ig^2 C_f \int_q \gamma^\sigma S(q_1)\Gamma^\nu(q, p_1, -q_1)\Delta_{\nu\sigma}(q)\right]}_{i\Sigma(p_1)}\gamma_5 \tag{4.9}$$

$$+ \underbrace{ig^2 C_f \int_q \gamma^\sigma S(q_1)\left[\Gamma^\nu(q, p_1, -q_1)\gamma_5 + \gamma_5\Gamma^\nu(q, p_2, -q_2)\right]\Delta_{\nu\sigma}(q)}_{\mathcal{V}(p_1,p_2)\text{: symmetry violating remainder}}. \tag{4.10}$$

Thus, one finally has that

$$P_\mu(a_5^\mu) = i\left[\Sigma(p_1)\gamma_5 + \gamma_5\Sigma(p_2)\right] + \mathcal{V}(p_1, p_2), \tag{4.11}$$

with the symmetry violating remainder $\mathcal{V}(p_1, p_2)$ given in Eq. (4.10). Clearly, in the RL approximation, $\mathcal{V}(p_1, p_2) \sim \gamma^\nu\gamma_5 + \gamma_5\gamma^\nu = 0$.

It is now apparent that the gluon-axial-vector vertex $G_5^{\mu\nu}$, depicted in Fig. 5, must provide the *symmetry-restoring* contribution that will annihilate precisely the term $\mathcal{V}(p_1, p_2)$. It turns out that this is indeed what happens, by virtue of the fundamental WTI satisfied by $G_5^{\mu\nu}$, namely the $[\mathrm{WTI}]_{\mathrm{G}_5}$ in Eq. (3.11). Indeed, using $[\mathrm{WTI}]_{\mathrm{G}_5}$ and the expression for (b_5^μ) given in Eq. (4.5), we obtain directly

$$\begin{aligned} P_\mu(b_5^\mu) = & -ig^2 C_f \int_q \gamma^\sigma S(q_1) \big[\Gamma^\nu(q, p_1, -q_1)\gamma_5 \\ & +\gamma_5\Gamma^\nu(q, p_2, -q_2)\big] \Delta_{\nu\sigma}(q) \\ = & -\mathcal{V}(p_1, p_2). \end{aligned} \tag{4.12}$$

Therefore, after the inclusion of the vertex $G_5^{\mu\nu}$, the key $[\mathrm{WTI}]_{\Gamma_5}$ is exactly fulfilled at the level of the SDE for Γ_5^μ,

$$-P_\mu\left[\gamma_5\gamma^\mu + (a_5^\mu) + (b_5^\mu)\right] = S^{-1}(p_1)\gamma_5 + \gamma_5 S^{-1}(p_2). \tag{4.13}$$

Note that the essence of this result was already stated in [124], where the need of a vertex satisfying $[\mathrm{WTI}]_{\mathrm{G}_5}$ in order to preserve the axial WTI at the level of the Γ_5^μ SDE was duly recognized.

5 Dynamical realization of the chiral limit

As explained in Sect. 3, the pivotal relations in Eqs. (3.9) and (3.10) are a direct consequence of the $[\mathrm{WTI}]_{\Gamma_5}$. Given that, as shown in detail in Sect. 4, the SDE that governs the vertex Γ_5^μ satisfies the $[\mathrm{WTI}]_{\Gamma_5}$ *exactly*, it is natural to expect that there will be a dynamical realization of Eqs. (3.9) and (3.10), recovered by taking the $P \to 0$ limit of diagrams (a_5^μ) and (b_5^μ) in Fig. 8. This particular demonstration is nontrivial, and furnishes additional valuable insights into this subject; the aim of this section is to show in detail how this important result emerges both within the RL approximation and in the general case.

5.1 Chiral limit in the RL approximation

In order to fix the ideas, it is instructive to revert to the simpler case of the RL approximation, which involves only diagram (a_5^μ), with $\Gamma_\nu(q, r, -p) \to \gamma_\nu$, *i.e.*,

$$\Gamma_5^\mu = \gamma_5\gamma^\mu + (a_5^\mu)_{\mathrm{RL}}, \tag{5.1}$$

with

$$\begin{aligned} (a_5^\mu)_{\mathrm{RL}} = & -ig^2 C_f \int_q \gamma^\sigma S(q_1)\Gamma_5^\mu(P, q_2, -q_1) \\ & S(q_2)\gamma^\nu \Delta_{\nu\sigma}(q). \end{aligned} \tag{5.2}$$

When we contract both sides of Eq. (5.1) by P_μ and take the limit $P \to 0$ (with $p_1 = p_2 := p$), the corresponding pole residues are isolated, while the tree-level term is annihilated. In particular, using Eqs. (3.5) and (3.8) on both sides, we get

$$\begin{aligned} [\chi_1(p^2) + \chi_3(p^2)\not{p}]\gamma_5 = & -ig^2 C_f \int_q \gamma^\sigma S(q)\left[\chi_1(q^2) + \chi_3(q^2)\not{q}\right]\gamma_5 \\ & S(q)\gamma^\nu \Delta_{\nu\sigma}(q-p), \end{aligned} \tag{5.3}$$

where we have shifted the integration variable $q \to p + q$.

Using the basic property $\gamma_5 S(q) = S(-q)\gamma_5$, and the elementary result

$$S(q)S(-q) = -c(q^2), \tag{5.4}$$

with the function $c(q^2)$ defined in Eq. (2.3), we find

$$\begin{aligned} \chi_1(p^2) + \chi_3(p^2)\not{p} = & -ig^2 C_f \int_q \gamma^\sigma c(q^2)\left[\chi_1(q^2) + \chi_3(q^2)\not{q}\right] \\ & \gamma^\nu \Delta_{\nu\sigma}(q-p), \end{aligned} \tag{5.5}$$

where the γ_5 has been canceled from both sides.

It is now elementary to isolate two separate equations from Eq. (5.5), by taking appropriate Dirac traces, namely

$$\chi_1(p^2) = -\frac{ig^2 C_f}{4} \int_q c(q^2)\chi_1(q^2)\mathrm{Tr}\left[\gamma^\sigma\gamma^\nu\right]\Delta_{\nu\sigma}(q-p), \tag{5.6}$$

and

$$\begin{aligned} p^2\chi_3(p^2) = & \frac{ig^2 C_f}{4} \int_q c(q^2)\chi_3(q^2)\mathrm{Tr}\left[\not{p}\gamma^\sigma\not{q}\gamma^\nu\right] \\ & \Delta_{\nu\sigma}(q-p). \end{aligned} \tag{5.7}$$

It is clear at this point that Eq. (5.7) admits the trivial solution $\chi_3(p^2) = 0$, in compliance with Eq. (3.10). In addition, substituting Eq. (3.9) into Eq. (5.6), and using that $b(q^2) = c(q^2)B(q^2)$ [see Eq. (2.3)], one recovers precisely the dynamical equation governing $B(p^2)$ in the RL approximation, namely the second relation in Eq. (2.20). Thus, the dynamical Eqs. (5.6) and (5.7), derived from the SDE of the axial-vector vertex, are fully consistent with the symmetry relations (3.9) and (3.10).

5.2 Chiral limit with full quark-gluon vertex

Let us consider again the SDE of Eq. (4.3)

$$\Gamma_5^\mu = \gamma_5\gamma^\mu + (a_5^\mu) + (b_5^\mu), \tag{5.8}$$

with (a_5^μ) and (b_5^μ) given by Eqs. (4.4) and (4.5), now maintaining inside (a_5^μ) the full structure of the quark-gluon vertex $\Gamma_\nu(q, r, -p)$, as given by Eq. (2.8).

Next, we contract both sides of Eq. (5.8) by P_μ, and take the limit $P \to 0$. Evidently, the l.h.s. is exactly the same as that of Eq. (5.3). On the r.h.s., the leading contributions of (a_5^μ) and (b_5^μ) are generated by the pole part of the vertices Γ_5^μ and $G_5^{\mu\nu}$, respectively, *i.e.*,

$$\lim_{P\to 0} P_\mu(a_5^\mu) = -ig^2 C_f \int_q \gamma^\sigma S(q)\left[\chi_1(q^2) + \chi_3(q^2)q\!\!\!/\right] \gamma_5 S(q)\Gamma^\nu(q', p, -q)\Delta_{\nu\sigma}(q'), \tag{5.9}$$

$$\lim_{P\to 0} P_\mu(b_5^\mu) = -2ig^2 C_f \int_q \gamma^\sigma S(q)\Gamma_2^\nu (q', p, -q)\Delta_{\nu\sigma}(q')\gamma_5, \tag{5.10}$$

where we have used Eq. (3.14) to arrive at Eq. (5.10), and we have set $q' = q - p$.

Using Eq. (5.4), the decomposition of the quark-gluon vertex in Eq. (2.10), and the relation in Eq. (2.12), we may bring the γ_5 of Eq. (5.9) all the way to the right, namely

$$\lim_{P\to 0} P_\mu(a_5^\mu) = ig^2 C_f \int_q \gamma^\sigma c(q^2)\left[\chi_1(q^2) + \chi_3(q^2)q\!\!\!/\right] \left[\Gamma_2^\nu(q', p, -q) - \Gamma_1^\nu(q', p, -q)\right]\Delta_{\nu\sigma}(q')\gamma_5. \tag{5.11}$$

Therefore, after canceling the γ_5 from both sides, we arrive at the result

$$\chi_1(p^2) + \chi_3(p^2)p\!\!\!/ = (a_\chi) + (b_\chi), \tag{5.12}$$

with

$$(a_\chi) = ig^2 C_f \int_q \gamma^\sigma c(q^2)\left[\chi_1(q^2) + \chi_3(q^2)q\!\!\!/\right] \left[\Gamma_2^\nu(q', p, -q) - \Gamma_1^\nu(q', p, -q)\right]\Delta_{\nu\sigma}(q'), \tag{5.13}$$

$$(b_\chi) = -2ig^2 C_f \int_q \gamma^\sigma S(q)\Gamma_2^\nu(q', p, -q)\Delta_{\nu\sigma}(q'), \tag{5.14}$$

which may be diagrammatically interpreted as shown in Fig. 9.

The two individual equations for $\chi_1(p^2)$ and $\chi_3(p^2)$ are given by

$$4\chi_1(p^2) = \mathrm{Tr}(a_\chi) + \mathrm{Tr}(b_\chi), \tag{5.15}$$

$$4p^2\chi_3(p^2) = \mathrm{Tr}\left[p\!\!\!/(a_\chi)\right] + \mathrm{Tr}\left[p\!\!\!/(b_\chi)\right], \tag{5.16}$$

It is relatively straightforward to determine the four traces appearing in Eqs. (5.15) and (5.16), namely

$$\begin{aligned}\mathrm{Tr}(a_\chi) &= ig^2 C_f \int_q c(q^2)\chi_3(q^2)\mathrm{Tr}\left[\gamma^\sigma q\!\!\!/\,\Gamma_2^\nu(q', p, -q)\right]\Delta_{\nu\sigma}(q') \\ &\quad - ig^2 C_f \int_q c(q^2)\chi_1(q^2)\mathrm{Tr}\left[\gamma^\sigma \Gamma_1^\nu(q', p, -q)\right]\Delta_{\nu\sigma}(q'), \\ \mathrm{Tr}(b_\chi) &= -2ig^2 C_f \int_q \mathrm{Tr}\left[\gamma^\sigma S(q)\Gamma_2^\nu(q', p, -q)\right]\Delta_{\nu\sigma}(q')\end{aligned} \tag{5.17}$$

$$= -2ig^2 C_f \int_q a(q^2)\mathrm{Tr}\left[\gamma^\sigma q\!\!\!/\,\Gamma_2^\nu(q', p, -q)\right]\Delta_{\nu\sigma}(q'), \tag{5.18}$$

and

$$\begin{aligned}\mathrm{Tr}\left[p\!\!\!/(a_\chi)\right] &= ig^2 C_f \int_q c(q^2)\chi_1(q^2)\mathrm{Tr}\left[p\!\!\!/\gamma^\sigma \Gamma_2^\nu(q', p, -q)\right]\Delta_{\nu\sigma}(q') \\ &\quad - ig^2 C_f \int_q c(q^2)\chi_3(q^2)\mathrm{Tr}\left[p\!\!\!/\gamma^\sigma q\!\!\!/\,\Gamma_1^\nu(q', p, -q)\right]\Delta_{\nu\sigma}(q'), \\ \mathrm{Tr}\left[p\!\!\!/(b_\chi)\right] &= -2ig^2 C_f \int_q \mathrm{Tr}\left[p\!\!\!/\gamma^\sigma S(q)\Gamma_2^\nu(q', p, -q)\right]\Delta_{\nu\sigma}(q')\end{aligned} \tag{5.19}$$

$$= -2ig^2 C_f \int_q b(q^2)\mathrm{Tr}\left[p\!\!\!/\gamma^\sigma \Gamma_2^\nu(q', p, -q)\right]\Delta_{\nu\sigma}(q'). \tag{5.20}$$

Note that in computing $\mathrm{Tr}(b_\chi)$ and $\mathrm{Tr}\left[p\!\!\!/(b_\chi)\right]$ we have used the parametrization introduced in Eq. (2.2), setting $S(q) = a(q^2)q\!\!\!/ + b(q^2)$.

We are now in a position to verify that the system in Eqs. (5.15) and (5.16) is compatible with the key symmetry relations (3.9) and (3.10), namely $\{\chi_1(p^2), \chi_3(p^2)\} = \{2B(p^2), 0\}$.

To that end, we first focus on Eq. (5.16), and note that the substitution $\chi_1(q^2) = 2B(q^2)$ into the first term of $\mathrm{Tr}\left[p\!\!\!/(a_\chi)\right]$ in Eq. (5.19) triggers a crucial cancellation. Specifically, using Eq. (2.3), we have that $c(q^2)\chi_1(q^2) = 2c(q^2)B(q^2) = 2b(q^2)$, and so $\mathrm{Tr}\left[p\!\!\!/(b_\chi)\right]$ cancels exactly against this term, namely

$$\mathrm{Tr}\left[p\!\!\!/(a_\chi)\right] + \mathrm{Tr}\left[p\!\!\!/(b_\chi)\right] = ig^2 C_f \int_q c(q^2)\chi_3(q^2)\mathrm{Tr}\left[\gamma^\sigma q\!\!\!/\,\Gamma_2^\nu(q', p, -q)\right]\Delta_{\nu\sigma}(q'). \tag{5.21}$$

Thus, by virtue of Eq. (5.21), Eq. (5.16) becomes

$$4p^2\chi_3(p^2) = -ig^2 C_f \int_q c(q^2)\chi_3(q^2)\mathrm{Tr}\left[p\!\!\!/\gamma^\sigma q\!\!\!/\,\Gamma_1^\nu(q', p, -q)\right]\Delta_{\nu\sigma}(q'), \tag{5.22}$$

which obviously admits the trivial solution $\chi_3(p^2) = 0$, as dictated by the symmetry. Note that the inclusion of graph (b_5^μ) is instrumental for achieving this result; indeed, the contribution of diagram (a_5^μ) alone fails to vanish when $\chi_3 = 0$,

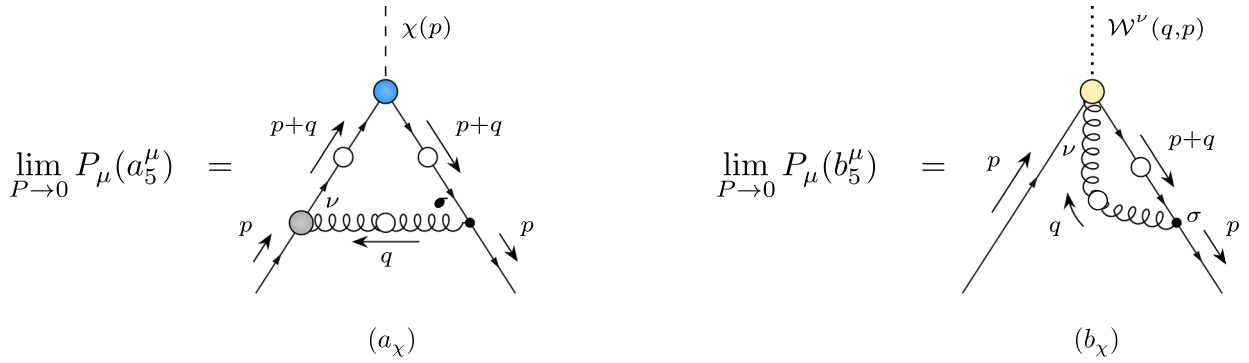

Fig. 9 Diagrammatic representation of (a_χ) and (b_χ): the contributions of diagrams (a_5^μ) and (b_5^μ), respectively, in the limit $P \to 0$

because of the term $\int_q c(q^2)\chi_1(q^2)\mathrm{Tr}\left[p\!\!/\gamma^\sigma \Gamma_2^\nu(q', p, -q)\right] \Delta_{\nu\sigma}(q')$, which vanishes in the RL (because $\Gamma_2^\nu = 0$, trivially), but is nonvanishing in general.

Turning to Eq. (5.15), and substituting $\{\chi_1(p^2), \chi_3(p^2)\} = \{2B(p^2), 0\}$ into Eqs. (5.17) and (5.18), we arrive at

$$B(p^2) = -\frac{ig^2 C_f}{4}\int_q b(q^2)\mathrm{Tr}\left[\gamma^\sigma \Gamma_1^\nu(q', p, -q)\right]\Delta_{\nu\sigma}(q') - \frac{ig^2 C_f}{4}\int_q a(q^2)\mathrm{Tr}\left[\gamma^\sigma q\!\!/\, \Gamma_2^\nu(q', p, -q)\right]\Delta_{\nu\sigma}(q'), \tag{5.23}$$

which is precisely Eq. (2.18), the dynamical equation for $B(p^2)$ obtained from the gap equation.

The results of this section demonstrate clearly that the two key equations controlling the axial-vector vertex, namely its SDE and its WTI, are completely compatible with each other.

6 Unfolding the $G_5^{\mu\nu}$: one-loop dressed approximation

Up until this point, the SDE for the gluon-axial-vector vertex $G_5^{\mu\nu}$ has been treated exactly, without resorting to any type of approximation. However, for practical purposes, we need either a diagrammatic expansion for $G_5^{\mu\nu}$, or an Ansatz that capitalizes on the $[\mathrm{WTI}]_{\mathrm{G_5}}$ that this vertex satisfies, see discussion at the end of this section.

Opting for the former possibility, in what follows we consider the *"one-loop dressed"* approximation to $G_5^{\mu\nu}$, consisting of one-loop diagrams that contain fully-dressed propagators and vertices, as shown in Figs. 10 and 11. Note that this type of truncation has already been discussed in Sect. 2, in the context of the SDE for the quark-gluon vertex. Therefore, in complete analogy to the $\Gamma_\mu^{(1)}$ introduced in Eq. (2.13), the gluon-axial-vector vertex emerging from this approximation will be denoted by $G_{5\mu\nu}^{(1)}$.

The vertex $G_{5\mu\nu}^{(1)}$ can be expressed as

$$G_{5\mu\nu}^{(1)} = \mathcal{A}_{5\mu\nu} + \mathcal{B}_{5\mu\nu}, \tag{6.1}$$

where

$$\mathcal{A}_5^{\mu\nu} := d_1^{\mu\nu} + d_2^{\mu\nu} + g_1^{\mu\nu} + g_2^{\mu\nu} + g_3^{\mu\nu},$$
$$\mathcal{B}_5^{\mu\nu} := d_3^{\mu\nu} + h_1^{\mu\nu} + h_2^{\mu\nu}, \tag{6.2}$$

and $d_i^{\mu\nu}$, $g_i^{\mu\nu}$ and $h_i^{\mu\nu}$ label the contributions shown in Figs. 10 and 11. The obvious distinction between these two sets is that the diagrams belonging to $\mathcal{A}_5^{\mu\nu}$ do not contain a three-gluon vertex, while those of $\mathcal{B}_5^{\mu\nu}$ do; we will therefore refer to these two sets as "abelian" and "non-abelian", respectively. In addition, note that the susbet of diagrams shown in Fig. 11 contain the vertex $G_5^{\mu\nu}$ itself as their basic ingredient.

We now turn to the key question of what happens to the $[\mathrm{WTI}]_{\mathrm{G_5}}$ when $G_{5\mu\nu}$ is approximated by Eqs. (6.1) and (6.2), *i.e.*, $G_{5\mu\nu} \to G_{5\mu\nu}^{(1)}$. In order to address this issue, we will contract by P_μ all diagrams given by Figs. 10 and 11. Quite interestingly, the answer that will emerge is *precisely* the r.h.s. of $[\mathrm{WTI}]_{\mathrm{G_5}}$, but with $\Gamma_\nu \to \Gamma_\nu^{(1)}$. In other words, the one-loop dressed versions of $G_{5\mu\nu}$ and Γ_ν are connected by the correct WTI.

We start by considering the set of abelian diagrams belonging to the set $\mathcal{A}_5^{\mu\nu}$. Contracting by P_μ and using $[\mathrm{WTI}]_{\mathrm{G_5}}$, we write

$$P_\mu d_1^{\mu\nu} = -L_1^\nu - L_3^\nu, \qquad P_\mu d_2^{\mu\nu} = -L_2^\nu - L_4^\nu, \tag{6.3}$$

where

$$L_1^\nu = g^2\kappa_a \int_k \Gamma^\beta(-k, k_1', -q_1)\gamma_5 S(k_2')\Gamma^\nu(q, k_2, -k_2') S(k_2)\Gamma^\alpha(k, p_2, -r_2)\Delta_{\alpha\beta}(k),$$
$$L_2^\nu = g^2\kappa_a \int_k \Gamma^\beta(-k, k_1', -q_1) S(k_1')\Gamma^\nu(q, k_1, -k_1') S(k_1)\gamma_5\Gamma^\alpha(k, p_2, -k_2)\Delta_{\alpha\beta}(k),$$
$$L_3^\nu = g^2\kappa_a \int_k \Gamma^\beta(-k, k_1', -q_1) S(k_1')\gamma_5\Gamma^\nu(q, k_2, -k_2') S(k_2)\Gamma^\alpha(k, p_2, -k_2)\Delta_{\alpha\beta}(k),$$
$$L_4^\nu = g^2\kappa_a \int_k \Gamma^\beta(-k, k_1', -q_1) S(k_1')\Gamma^\nu(q, k_1, -k_1') \times\gamma_5 S(k_2)\Gamma^\alpha(k, p_2, -k_2)\Delta_{\alpha\beta}(k), \tag{6.4}$$

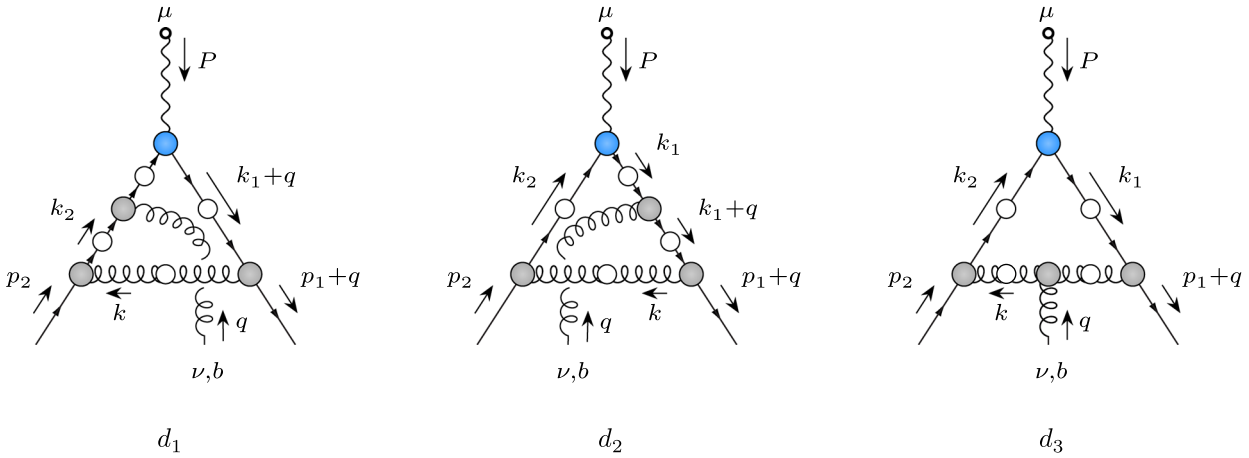

Fig. 10 One-loop dressed diagrams contributing to the gluon-axial-vector vertex SDE, in the lowest-order of its dressed-loop expansion, and not involving $G_5^{\mu\nu}$ itself

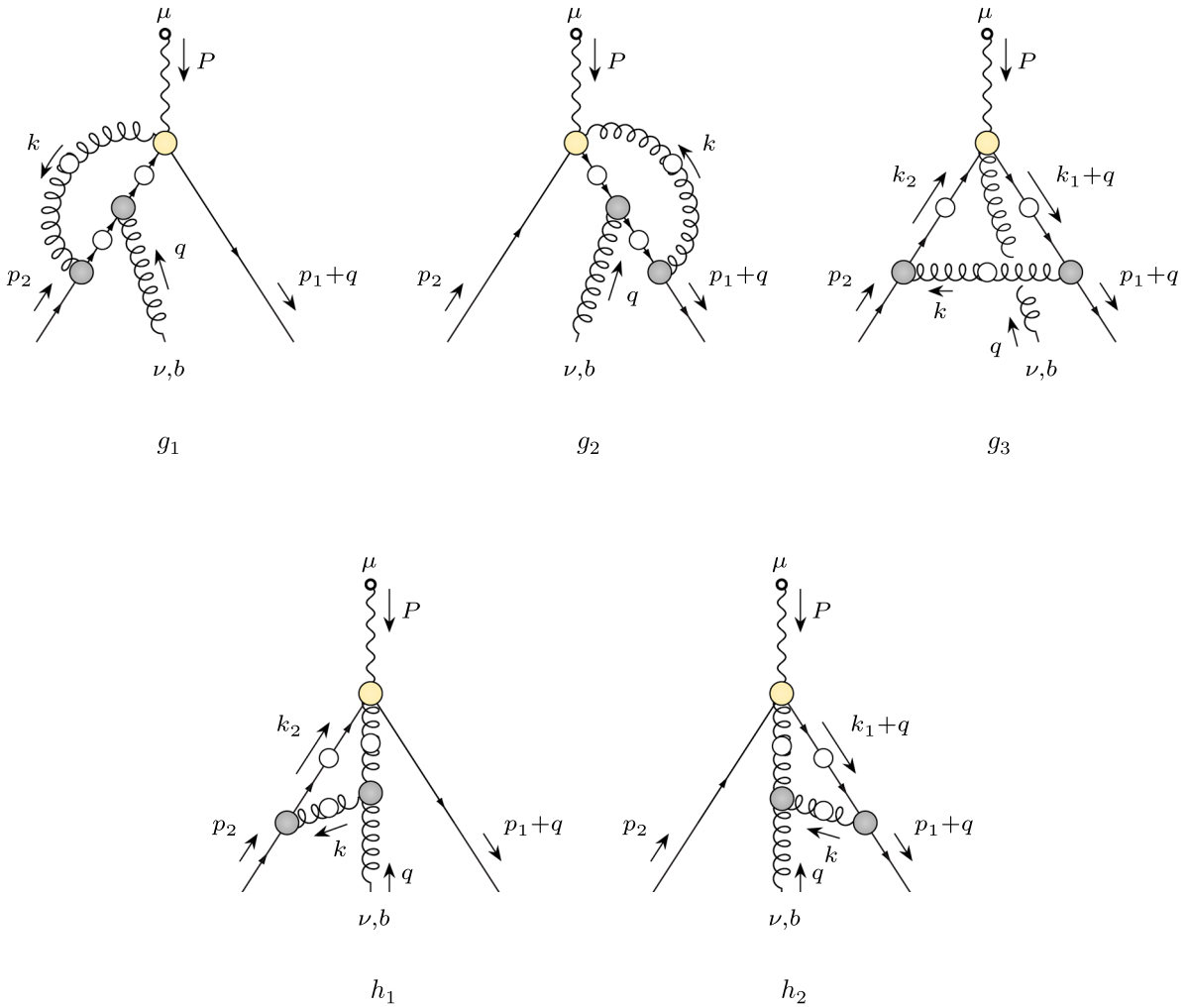

Fig. 11 One-loop dressed diagrams contributing to the gluon-axial-vector vertex SDE in the lowest-order of its dressed-loop expansion, and involving $G_5^{\mu\nu}$ itself

with $k_i' := k_i + q$ and $\kappa_a := C_f - C_A/2$.

A similar calculation may be carried out for the diagrams $\{g\}_i$, *i.e.*,

$$\begin{aligned}
P_\mu g_1^{\mu\nu} &= L_1^\nu + g^2\kappa_a \int_k \gamma_5\Gamma^\beta(-k,k_2',-q_2)\\
&\quad S(k_2')\Gamma^\nu(q,k_2,-k_2')S(k_2)\Gamma^\alpha(k,p_2,-k_2)\Delta_{\alpha\beta}(k),\\
P_\mu g_2^{\mu\nu} &= L_2^\nu + g^2\kappa_a \int_k \Gamma^\beta(-k,k_1',-q_1)\\
&\quad S(k_1')\Gamma^\nu(q,k_1,-k_1')S(k_1)\Gamma^\alpha(k,p_1,-k_1)\gamma_5\Delta_{\alpha\beta}(k),\\
P_\mu g_3^{\mu\nu} &= L_3^\nu + L_4^\nu.
\end{aligned} \tag{6.5}$$

When these five contributions are added up, a number of key cancellations takes place, leaving us with two terms, namely

$$\begin{aligned}
P_\mu \mathcal{A}_5^{\mu\nu} &= \underbrace{g^2\kappa_a \int_k \Gamma^\beta(-k,k_1',-q_1)S(k_1')\Gamma^\nu(q,k_1,-k_1')S(k_1)\Gamma^\alpha(k,p_1,-k_1)\Delta_{\alpha\beta}(k)\,\gamma_5}_{(c_1^\nu)\text{ of Fig.4 at }\{r,-p\}=\{p_1,-q_1\}}\\
&\quad +\gamma_5\,\underbrace{g^2\kappa_a \int_k \Gamma^\beta(-k,k_2',-q_2)S(k_2')\Gamma^\nu(q,k_2,-k_2')S(k_2)\Gamma^\alpha(k,p_2,-k_2)\Delta_{\alpha\beta}(k)}_{(c_1^\nu)\text{ of Fig.4 at }\{r,-p\}=\{p_2,-q_2\}},
\end{aligned} \tag{6.6}$$

or, diagrammatically,

$$-iP_\mu \mathcal{A}_5^{\mu\nu} = \left(\quad\right)\gamma_5 \quad + \quad \gamma_5\left(\quad\right). \tag{6.7}$$

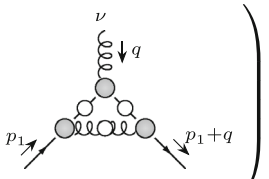

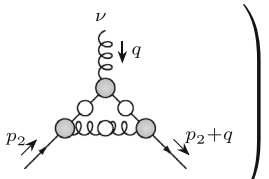

Next, we turn to the non-abelian subset $\mathcal{B}_5^{\mu\nu}$, and follow completely analogous steps. In particular,

$$P_\mu d_3^{\mu\nu} = -L_5^\nu - L_6^\nu, \tag{6.8}$$

where

$$\begin{aligned}
L_5^\nu &= -ig^2\kappa_b \int_k \Gamma^\beta(-k',k_1,-q_1)\gamma_5 S(k_2)\Gamma^\alpha(k,p_2,-k_2)\\
&\quad \Gamma^{\nu\rho\sigma}(q,-k,k')\Delta_{\alpha\rho}(k)\Delta_{\sigma\beta}(k'),\\
L_6^\nu &= -ig^2\kappa_b \int_k \Gamma^\beta(-k',k_1,-q_1)S(k_1)\gamma_5\Gamma^\alpha(k,p_2,-k_2)\\
&\quad \Gamma^{\nu\rho\sigma}(q,-k,k')\Delta_{\alpha\rho}(k)\Delta_{\sigma\beta}(k'),
\end{aligned} \tag{6.9}$$

with $k' := k - q$ and $\kappa_b := iC_A/2$, and

$$\begin{aligned}
P_\mu h_1^{\mu\nu} &= L_5^\nu - ig^2\kappa_b \int_k \gamma_5\Gamma^\beta(-k',k_2,-q_2)S(k_2)\\
&\quad \Gamma^\alpha(k,p_2,-k_2)\Gamma^{\nu\rho\sigma}(q,-k,k')\Delta_{\alpha\rho}(k)\Delta_{\sigma\beta}(k'),
\end{aligned}$$

$$\begin{aligned}
P_\mu h_2^{\mu\nu} &= L_6^\nu - ig^2\kappa_b \int_k \Gamma^\beta(-k',k_1,-q_1)S(k_1)\Gamma^\alpha(k,p_1,-k_1)\\
&\quad \gamma_5\Gamma^{\nu\rho\sigma}(q,-k,k')\Delta_{\alpha\rho}(k)\Delta_{\sigma\beta}(k').
\end{aligned} \tag{6.10}$$

As in the abelian case, an extensive cancellation takes place when the terms in Eqs. (6.9) and (6.10) are summed up: the entire contribution given by $d_3^{\mu\nu}$ is exactly canceled by parts of $h_1^{\mu\nu}$ and $h_2^{\mu\nu}$, leaving us with

$$\begin{aligned}
-P_\mu \mathcal{B}_5^{\mu\nu} &= \underbrace{ig^2\kappa_b \int_k \Gamma^\beta(-k',k_1,-q_1)S(k_1)\Gamma^\alpha(k,p_1,-k_1)\Gamma^{\nu\rho\sigma}(q,-k,k')\Delta_{\alpha\rho}(k)\Delta_{\sigma\beta}(k')\,\gamma_5}_{(c_2^\nu)\text{ of Fig.4 at }\{r,-p\}=\{p_1,-q_1\}}\\
&\quad +\gamma_5\,\underbrace{ig^2\kappa_b \int_k \Gamma^\beta(-k',k_2,-q_2)S(k_2)\Gamma^\alpha(k,p_2,-k_2)\Gamma^{\nu\rho\sigma}(q,-k,k')\Delta_{\alpha\rho}(k)\Delta_{\sigma\beta}(k')}_{(c_2^\nu)\text{ of Fig.4 at }\{r,-p\}=\{p_2,-q_2\}},
\end{aligned} \tag{6.11}$$

or, diagrammatically,

$$-iP_\mu \mathcal{B}_5^{\mu\nu} =$$

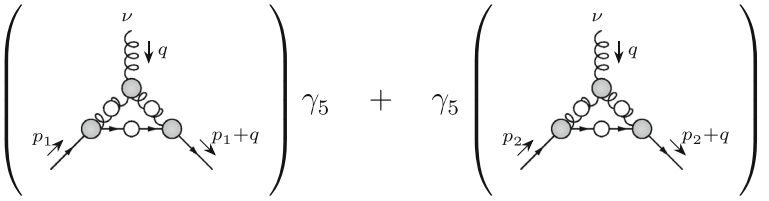

(6.12)

Evidently, now the non-abelian part of the exact $[\mathrm{WTI}]_{G_5}$ is formed, where the quark-gluon vertices are given by the non-abelian diagram of the SDE in Fig. 4.

Thus, combining Eqs. (6.7) and (6.12), we arrive at

$$-iP^\mu G^{(1)}_{5\mu\nu}(P,q,p_2,-q_1) =$$

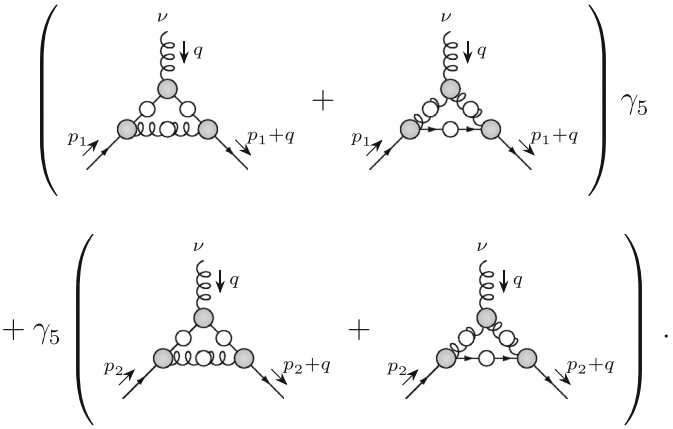

(6.13)

The result in Eq. (6.13) is rather striking: $G^{(1)}_{5\mu\nu}$, the one-loop dressed approximation of $G_{5\mu\nu}$, satisfies the $[\mathrm{WTI}]_{G_5}$ of Eq. (3.12), provided that the quark-gluon vertex is determined from the one-loop dressed version of its own SDE, shown in Fig. 4, to wit

$$-iP^\mu G^{(1)}_{5\mu\nu}(P,q,p_2,-q_1) = \Gamma^{(1)}_{Q\,\nu}(q,p_1,-q_1)\gamma_5 + \gamma_5\Gamma^{(1)}_{Q\,\nu}(q,p_2,-q_2). \tag{6.14}$$

Clearly, as already mentioned in Sect. 3, the tree-level contribution to the quark-gluon vertex may be added to the r.h.s. of Eq. (6.14) "for free", leading to

$$-iP^\mu G^{(1)}_{5\mu\nu}(P,q,p_2,-q_1) = \Gamma^{(1)}_{\nu}(q,p_1,-q_1)\gamma_5 + \gamma_5\Gamma^{(1)}_{\nu}(q,p_2,-q_2), \tag{6.15}$$

which is precisely the one-loop dressed realization of the $[\mathrm{WTI}]_{G_5}$.

We end this section by pointing out that, given the pivotal function of the vertex $G_5^{\mu\nu}$, it is important to consider alternative procedures for its determination. In particular, since the $[\mathrm{WTI}]_{G_5}$ is a most prominent feature of this vertex, one may opt for a gauge-technique type of construction [136–141]. This general method has been employed in numerous occasions in the literature, for a variety of vertices, see *e.g.*, [84,87,142]. Through this well-defined procedure, the non-transverse part of $G_5^{\mu\nu}$ may be reconstructed exactly from the $[\mathrm{WTI}]_{G_5}$, while the transverse part remains undetermined.

7 Symmetry-preserving truncation of the vertex Γ_5^μ

It is clear that the one-loop dressed approximation implemented at the level of $G_5^{\mu\nu}$ must be self-consistently incorporated into the SDE satisfied by Γ_5^μ, namely Eq. (4.3), together with Eqs. (4.4) and (4.5). In particular, the effective replacement $G_{5\mu\nu} \to G^{(1)}_{5\mu\nu}$ imposed at the level of graph (b_5^μ) must be accompanied by analogous adjustments, in order for the fundamental $[\mathrm{WTI}]_{G_5}$ to be maintained intact.

In order to elucidate this point, we remind the reader that, as shown in Sect. 4, the contribution of $G_5^{\mu\nu}$ inside (b_5^μ) is instrumental for canceling the symmetry violating contribution originating from (a_5^μ). This latter contribution, denoted by $\mathcal{V}(p_1,p_2)$, contains precisely the r.h.s. of the $[\mathrm{WTI}]_{G_5}$, see Eq. (4.10). Evidently, if the effective substitution $G_{5\mu\nu} \to G^{(1)}_{5\mu\nu}$ is carried out in graph (b_5^μ), then the one-loop version of the $[\mathrm{WTI}]_{G_5}$ in Eq. (6.15) is triggered. Therefore, in order for the aforementioned crucial cancel-

lation between the two graphs to still go through, the corresponding replacement $\Gamma_\nu \to \Gamma_\nu^{(1)}$ must be carried out in graph (a_5^μ).

Thus, one arrives at the following truncated version of the SDE for Γ_5^μ,

$$\Gamma_{1\nu}^{(1)}(q,p,-p-q) = \gamma_\nu + \Big[\quad + \quad \Big]_{\text{odd}} \,, \tag{7.4}$$

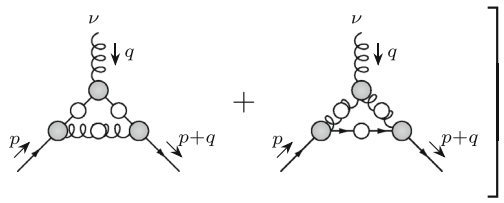

and

$$\Gamma_{2\nu}^{(1)}(q,p,-p-q) = \Big[\quad + \quad \Big]_{\text{even}} \,. \tag{7.5}$$

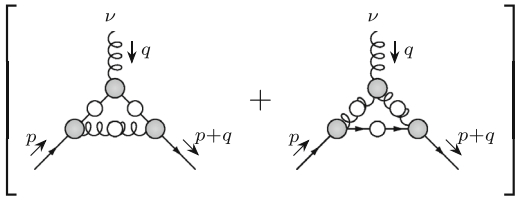

$$\Gamma_5^\mu = \gamma_5\gamma^\mu + (a_5^\mu) + (b_5^\mu), \tag{7.1}$$

where

$$(a_5^\mu) = -ig^2 C_f \int_q \gamma^\sigma S(q_1)\Gamma_5^\mu(P,q_2,-q_1)S(q_2) \Gamma_\nu^{(1)}(q,p_2,-q_2)\Delta_\sigma^\nu(q)\,, \tag{7.2}$$

$$(b_5^\mu) = -g^2 C_f \int_q \gamma^\sigma S(q_1) G_{5\nu}^{(1)\mu}(P,q,p_2,-q_1)\Delta_\sigma^\nu(q). \tag{7.3}$$

It is important to emphasize that, while graph (a_5^μ) in Eq. (7.2) is "one-loop dressed", (b_5^μ) is clearly "two-loop dressed", because the one-loop dressed $G_{5\mu\nu}^{(1)}$ is nested inside an additional integration over the gluon momentum q entering in it. In that sense, there is no self-consistent one-loop dressed treatment of the vertex Γ_5^μ, except within the RL approximation; within the confines of the present framework, any meaningful attempt to go beyond RL requires a beyond one-loop dressed treatment.

Let us now turn to the $[\text{WTI}]_{\Gamma_5}$ satisfied by the truncated vertex Γ_5^μ, defined through Eqs. (7.1),(7.2) and (7.3). It is clear from the above analysis that the $[\text{WTI}]_{\Gamma_5}$ is satisfied, provided that we carry out the substitution $\Gamma_\mu(q,p,-q) \to \Gamma_\mu^{(1)}(q-p,p,-q)$ inside Eq. (2.5), namely the equation defining the quark self-energy $\Sigma(p)$. Following steps identical to those of Sect. 2, we can derive the dynamical equations for the quark dressing functions $A(p^2)$ and $B(p^2)$. Those are exactly as in Eqs. (2.17) and (2.18), except for the substitution $\Gamma_1 \to \Gamma_1^{(1)}$ and $\Gamma_2 \to \Gamma_2^{(1)}$, defined by

8 Discussion and conclusions

In the present work we have developed a comprehensive approach that aims at a self-consistent treatment of the functional equations associated with the physics of mesons in the non-singlet sector.

The cornerstone of this formalism is the exact SDE of the axial-vector vertex Γ_5^μ, formulated from the viewpoint of the antiquark leg. This alternative re-organization of the quantum corrections is described in terms of a new vertex, denominated gluon-axial-vector vertex, and denoted by $G_5^{\mu\nu}$. This vertex is nested inside the SDE of Γ_5^μ, and satisfies its own WTI, which relates it to the quark-gluon vertex. As a result, the WTI of the axial-vector vertex is enforced directly at the level of the SDE. In particular, the gap equation governing the quark propagator appearing on the r.h.s. of this WTI involves the full quark-gluon vertex.

Information on the BSE of the pion is obtained by taking the limit $P \to 0$ of the above SDE, where P is the momentum of the axial-vector current. In particular, as it is well-known, when the chiral symmetry is dynamically broken, the axial-vector vertex possesses a (longitudinally coupled) pole in P^2, whose residue is identified with the BSA of the pion. By virtue of the aforementioned results, the known relation between the quark mass function, obtained from the

gap equation with a full Γ_μ, and the amplitude of the pion, is precisely fulfilled.

The developed framework offers a rather tight control on the interlocked equations describing symmetry and dynamics. As a result, it facilitates the design and implementation of simpler calculational methods. In particular, a concrete truncation scheme for the SDE-BSE system has been identified in Sect. 6, referred to as "one-loop dressed" approximation; it incorporates a completely nontrivial quark-gluon vertex Γ_μ, which is fully compatible with chiral symmetry, as expressed through the axial WTI.

It is worth pointing out that, throughout all algebraic manipulations of our analysis, the gluon propagator $\Delta_{\mu\nu}$ remained completely inert. Therefore, the formal aspects of this work persist for any value of the gauge-fixing parameter ξ, or even within gauge-fixing schemes other than the covariant gauges. Even though, for practical purposes, the Landau gauge is undoubtedly the standard choice, the validity of our considerations for arbitrary gauges is a welcome feature.

It is important to emphasize that our approach has been developed strictly in the limit of vanishing current quark masses. Its extension to arbitrary current masses is expected to proceed in a similar fashion, once the modifications to the key WTIs have been appropriately taken into account. In particular, in the presence of current masses, the WTIs contain additional terms involving the axial vertex Γ_5, see, *e.g.*, Eq. (11.217) in [74], or Eq. (14) in [133]. The vertex Γ_5 is associated with the axial current $j_5 = i\bar{\psi}\gamma_5\psi$, which satisfies the relation $\partial_\mu j_5^{\mu,a} = -2mt^a j_5$. We hope to present the completion of this task in the near future.

The practical implementation of the one-loop-dressed approximation mentioned above may not be easy to carry out, due to the presence of the vertex $G_5^{\mu\nu}$ inside some of the relevant diagrams, see Fig. 11. It turns out, however, that a further simplification is possible: one may omit the aforementioned diagrams, keeping only those in Fig. 10, provided that the SDE of the quark-gluon vertex, Fig. 4, is treated in the so-called "symmetric" limit. This treatment amounts to replacing the full momentum-dependence of the form factors in the quark-gluon SDE by the choice $q^2 = r^2 = p^2$, see, *e.g.*, [97]. This additional simplification is expected to lead to a more tractable version of the pion BSE, apt for numerical exploration. We expect to report progress in this direction in a forthcoming communication.

Funding The work of A.S.M., J.M.M.C. and J.P. is funded by the Spanish MICINN grants PID2020-113334GB-I00 and PID2023-151418NB-I00, the Generalitat Valenciana grant CIPROM/2022/66, and CEX2023-001292-S by MCIU/AEI. J.P. is supported in part by the EMMI visiting grant of the ExtreMe Matter Institute EMMI at the GSI, Darmstadt, Germany. J.M.P. is funded by the Deutsche Forschungsgemeinschaft (DFG, German Research Foundation) under Germany's Excellence Strategy EXC 2181/1 - 390900948 (the Heidelberg STRUCTURES Excellence Cluster) and the Collaborative Research Centre SFB 1225 - 273811115 (ISOQUANT).

Data Availability Statement This manuscript has no associated code/software. [Author's comment: Data sharing not applicable to this article as no datasets were generated or analysed during the current study.]

Code Availability Statement This manuscript has no associated code/software. [Author's comment: Code/Software sharing not applicable to this article as no code/software was generated or analysed during the current study.]

Appendix A: Derivation of the WTIs

In this Appendix we derive the key WTIs satisfied by the axial-vector vertex, Γ_5^μ, and the gluon-axial-vector vertex, $G_5^{\mu\nu}$, namely the $[\mathrm{WTI}]_{\Gamma_5}$ of Eq. (3.1) and the $[\mathrm{WTI}]_{G_5}$ of Eq. (3.11), respectively.

1. The $[\mathrm{WTI}]_{\Gamma_5}$

The starting point for the derivation of the required WTIs is the master formula given in Eq. (9.24) of [75]. In particular, for vanishing current quark mass, $m = 0$, we have

$$\begin{aligned}\partial_\mu^y \langle 0|T j_5^{\mu,a}(y)\varphi_1(x_1)\ldots\varphi_n(x_n)|0\rangle \\ = i\delta^4(y-x_1)\langle 0|T\frac{\partial\varphi_1(x_1)}{\partial\omega_{5\alpha}(x_1)}\cdots\varphi_n(x_n)|0\rangle + \cdots \\ + i\delta^4(y-x_n)\langle 0|T\varphi_1(x_1)\cdots\frac{\partial\varphi_n(x_n)}{\partial\omega_{5\alpha}(x_n)}|0\rangle,\end{aligned} \tag{A.1}$$

where the axial-vector current, $j_5^{\mu,a}(x)$, is given by

$$j_5^{\mu,a}(x) = \bar{\psi}(x)\gamma_5\gamma^\mu t^a\psi(x); \tag{A.2}$$

where t^a are the generators of flavour $SU(N_f)$ algebra, *e.g.*, the Gell-Mann matrices for $N_f = 3$; the φ_i represent field operators of arbitrary kind, ∂_μ^y is the derivative with respect to the spacetime variable y, the T denotes the standard time-ordering operator, and $\omega_{5\alpha}(x)$ is the angle of a local chiral transformation.

We now specialize Eq. (A.1) to the case $n = 2$, where $\varphi_1(x_1) = \psi(x_1)$ and $\varphi_1(x_2) = \bar{\psi}(x_2)$. To that end, we consider a local chiral transformation of the quark fields $\psi(x)$

and $\bar{\psi}(x)$ [73]

$$\delta\psi(x) = i\omega_{5\alpha}(x)\gamma_5 t^a\psi(x), \quad \delta\bar{\psi}(x) = i\omega_{5\alpha}(x)\bar{\psi}(x)\gamma_5 t^a, \tag{A.3}$$

and therefore,

$$\frac{\partial\psi(x)}{\partial\omega_{5\alpha}(x)} = i\gamma_5 t^a\psi(x), \quad \frac{\partial\bar{\psi}(x)}{\partial\omega_{5\alpha}(x)} = i\bar{\psi}(x)\gamma_5 t^a. \tag{A.4}$$

Thus, using Eq. (A.4), and suppressing isospin indices, we have

$$\begin{aligned}&\partial^y_\mu\langle 0|T j^\mu_5(y)\psi(x_1)\bar{\psi}(x_2)|0\rangle\\ &\quad = -\delta^4(y-x_1)\gamma_5\langle 0|T\psi(x_1)\bar{\psi}(x_2)|0\rangle\\ &\quad\quad -\delta^4(y-x_2)\langle 0|T\psi(x_1)\bar{\psi}(x_2)|0\rangle\gamma_5.\end{aligned} \tag{A.5}$$

The Fourier transform of the correlation function $\widetilde{\Gamma}^\mu_5(y, x_1, x_2) := \langle 0|T j^\mu_5(y)\psi(x_1)\bar{\psi}(x_2)|0\rangle$ defines the connected axial-vector vertex, $\widetilde{\Gamma}^\mu_5(P, p_2, -p_1)$, namely

$$\begin{aligned}&(2\pi)^4\delta^4(P+p_2-p_1)\widetilde{\Gamma}^\mu_5(P, p_2, -p_1)\\ &\quad = \int_{-\infty}^{+\infty} d^4y\, d^4x_1\, d^4x_2\, e^{i(Py-p_1x_1+p_2x_2)}\widetilde{\Gamma}^\mu_5(y, x_1, x_2),\end{aligned} \tag{A.6}$$

while the Fourier transform for the quark propagator is given by

$$\begin{aligned}(2\pi)^4\delta^4(p+q)iS(p) = \int_{-\infty}^{+\infty} d^4x_1 d^4x_2 e^{i(px_1+qx_2)}\\ \langle 0|T\psi(x_1)\bar{\psi}(x_2)|0\rangle.\end{aligned} \tag{A.7}$$

We next integrate both sides of Eq. (A.5) by $\int d^4y\, d^4x_1\, d^4x_2\, e^{i(Py-p_1x_1+p_2x_2)}$. Then, on the l.h.s. we carry out the standard integration by parts, which brings in a $-iP_\mu$, while on the r.h.s. we simply recover two Fourier transforms of the quark propagator. Thus, we get

$$P_\mu\widetilde{\Gamma}^\mu_5(P, p_2, -p_1) = \gamma_5 S(p_1) + \gamma_5 S(p_2). \tag{A.8}$$

The amputated axial-vector vertex $\Gamma^\mu_5(P, p_2, -p_1)$ is defined as

$$\widetilde{\Gamma}^\mu_5(P, p_2, -p_1) = iS(p_1)\Gamma^\mu_5(P, p_2, -p_1)iS(p_2), \tag{A.9}$$

and, therefore, from Eq. (A.8) we get

$$-P^\mu\Gamma^\mu_5(P, p_2, -p_1) = S^{-1}(p_1)\gamma_5 + \gamma_5 S^{-1}(p_2), \tag{A.10}$$

namely the $[\text{WTI}]_{\Gamma_5}$ in Eq. (3.1).

2. The $[\text{WTI}]_{G_5}$

In the case of the gluon-axial-vector vertex $G^{\mu\nu}_5(P, q, p_2, -q_1)$, where $q_1 = p_1 + q$, we consider again the master formula of Eq. (A.1) for $n = 3$, choosing $\varphi_1(x_1) = \psi(x_1)$, $\varphi_1(x_2) = \bar{\psi}(x_2)$, and $\varphi_1(x_3) = A^\nu_b(x_3)$, where $A^\nu_b(x_3)$ is a gluon field. Since the gluon field is invariant under the chiral transformation, we have $\partial A^\nu_b(x_3)(x)/\partial\omega_{5\alpha}(x) = 0$. Thus, Eq. (A.1) yields (we suppress color indices)

$$\begin{aligned}&\partial^y_\mu\langle 0|T j^\mu_5(y)\psi(x_1)\bar{\psi}(x_2)A^\nu(x_3)|0\rangle\\ &\quad = -\delta^4(y-x_1)\gamma_5\langle 0|T\psi(x_1)\bar{\psi}(x_2)A^\nu(x_3)|0\rangle\\ &\quad\quad -\delta^4(y-x_2)\langle 0|T\psi(x_1)\bar{\psi}(x_2)A^\nu(x_3)|0\rangle\gamma_5.\end{aligned} \tag{A11}$$

The Fourier transform of the connected $\widetilde{\mathbb{G}}^{\mu\nu}_5(P, q, p_2, -q_1)$ is given by

$$\begin{aligned}&(2\pi)^4\delta^4(P+q+p_2-q_1)\widetilde{\mathbb{G}}^{\mu\nu}_5(P, q, p_2, -q_1)\\ &\quad = \int_{-\infty}^{+\infty} d^4y\, d^4x_1\, d^4x_2\, d^4x_3 e^{i(Py-q_1x_1+p_2x_2+qx_3)}\\ &\quad\times\langle 0|T j^\mu_5(y)\psi(x_1)\bar{\psi}(x_2)A^\nu(x_3)|0\rangle,\end{aligned} \tag{A12}$$

whereas the Fourier transform of the connected quark-gluon vertex $\widetilde{\Gamma}^\nu(q, r, -p)$ is given by

$$\begin{aligned}&(2\pi)^4\delta^4(q+r-p)\widetilde{\Gamma}^\nu(q, r, -p)\\ &\quad = \int_{-\infty}^{+\infty} d^4y\, d^4x_1\, d^4x_2\, e^{i(-px_1+rx_2+qx_3)}\langle 0|\psi(x_1)\bar{\psi}(x_2)\\ &\quad A^\nu(x_3)|0\rangle.\end{aligned} \tag{A13}$$

Using these relations, one obtains from Eq. (A11)

$$\begin{aligned}iP_\mu\widetilde{\mathbb{G}}^{\mu\nu}_5(P, q, p_2, -q_1) &= \gamma_5\widetilde{\Gamma}^\nu(q, p_1, -q_1)\\ &\quad +\widetilde{\Gamma}^\nu(q, p_2, -q_2)\gamma_5.\end{aligned} \tag{A14}$$

We next introduce the amputated $\mathbb{G}^{\mu\nu}_5$ and the amputated quark-gluon vertex Γ^ν, given by

$$\begin{aligned}\widetilde{\mathbb{G}}^{\mu\nu}_5(P, q, p_2, -q_1) &= \Delta^\nu_\rho(q)iS(q_1)\mathbb{G}^{\mu\rho}_5(P, q, p_2, -q_1)iS(p_2),\\ \widetilde{\Gamma}^\nu(q, r, -p) &= \Delta^\nu_\rho(q)iS(p)i\Gamma^\rho(q, r, -p)iS(r),\end{aligned} \tag{A15}$$

where S is the quark propagator defined in Eq. (A.7), and $\Delta_{\mu\nu}(q)$ is the gluon propagator.

Employing these definitions into Eq. (A14), and using that $q_i = q + p_i$ $(i = 1, 2)$, we get

$$\begin{aligned}&P_\mu\mathbb{G}^{\mu\nu}_5(P, q, p_2, -q_1) = \Gamma^\nu(q, p_1, -q_1)S(p_1)\gamma_5 S^{-1}(p_2)\\ &\quad +S^{-1}(q_1)\gamma_5 S(q_2)\Gamma^\nu(q, p_2, -q_2).\end{aligned} \tag{A16}$$

We next decompose $\mathbb{G}^{\mu\nu}_5$ into a 1PI part, denoted by $iG^{\mu\nu}_5$, and a 1PR part, denoted by $\mathcal{G}^{\mu\nu}_5$, *i.e.*, $\mathbb{G}^{\mu\nu}_5 = iG^{\mu\nu}_5 + \mathcal{G}^{\mu\nu}_5$. The contributions composing $\mathcal{G}^{\mu\nu}_5$ originate from diagrams (s_1) and (s_2) in Fig. 12, namely $\mathcal{G}^{\mu\nu}_5 = (s_1)^{\mu\nu}_5 + (s_2)^{\mu\nu}_5$, which are given by

$$(s_1)^{\mu\nu}_5 = \Gamma^\mu_5(P, p_2, -q_1)iS(q_2)i\Gamma^\nu(q, p_2, -q_2),$$

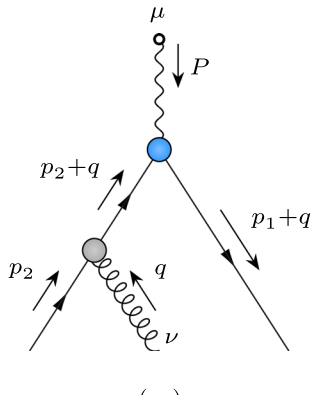

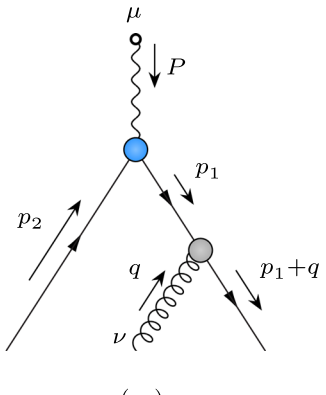

Fig. 12 1PR contributions to the amputated, connected part of the gluon-axial-vector function, $\mathbb{G}_5^{\mu\nu}$. The blue (gray) circles represent fully-dressed axial-vector (quark-gluon) vertices

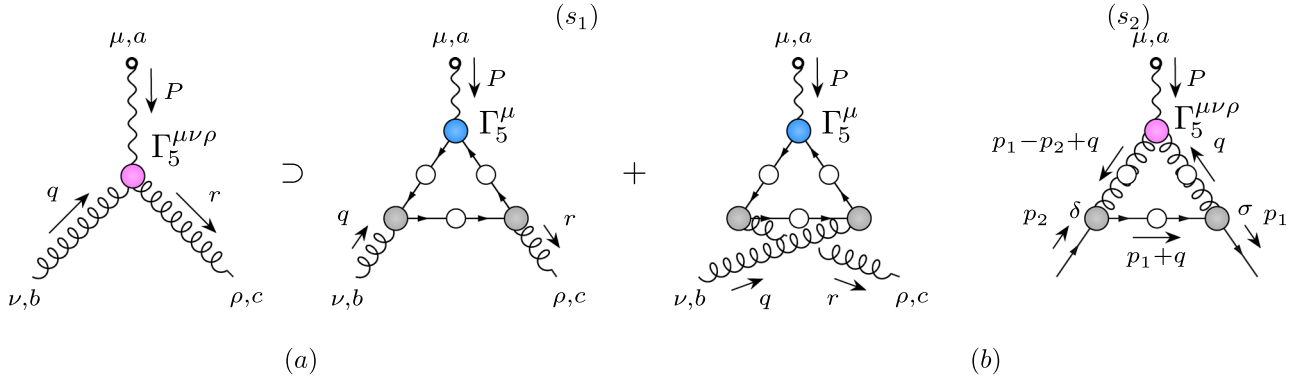

Fig. 13 *Left panel*: Gluon-gluon-axial-vector vertex; *Right panel*: Gluon-gluon-axial-vector vertex contribution to the singlet axial-vector vertex SDE

$$(s_2)_5^{\mu\nu} = i\Gamma^\nu(q, p_1, -q_1) i S(p_1) \Gamma_5^\mu(P, p_2, -p_1). \tag{A17}$$

Then, using Eq. (A.10), we find

$$\begin{aligned} P_\mu (s_1)_5^{\mu\nu} &= S^{-1}(q_1)\gamma_5 S(q_2) \\ &\quad \Gamma^\nu(q, p_2, -q_2) + \gamma_5 \Gamma^\nu(q, p_2, -q_2) \\ P_\mu (s_2)_5^{\mu\nu} &= \Gamma^\nu(q, p_1, -q_1)\gamma_5 \\ &\quad + \Gamma^\nu(q, p_1, -q_1) S(p_1)\gamma_5 S^{-1}(p_2). \end{aligned} \tag{A18}$$

We note now that the terms in Eq. (A18) contain the r.h.s. of Eq. (A16), namely

$$P_\mu \mathcal{G}_5^{\mu\nu} = \Gamma^\nu(q, p_1, -q_1)\gamma_5 + \gamma_5 \Gamma^\nu(q, p_2, -q_2) + [\text{r.h.s.}]_{(A16)} \tag{A19}$$

and therefore, from Eq. (A15) we get

$$i P_\mu G_5^{\mu\nu} + \Gamma^\nu(q, p_1, -q_1)\gamma_5 + \gamma_5 \Gamma^\nu(q, p_2, -q_2) = 0 \tag{A20}$$

which is precisely the $[\text{WTI}]_{G_5}$ of Eq. (3.11).

Appendix B: Flavour singlet and non-singlet currents

Throughout our construction we have considered the axial-vector current, which behaves as a non-singlet under flavour rotations $U \in SU(N_f)$. Specifically, the quark fields transform as

$$\psi(x) \to U\psi(x), \quad \bar\psi(x) \to \bar\psi(x) U^\dagger, \tag{B1}$$

and therefore, the axial-vector current defined in Eq. (A.2) transforms as

$$j_5^{\mu,a}(x) \to \bar\psi(x) U^\dagger \gamma_5 \gamma^\mu t^a U \psi(x). \tag{B2}$$

Since

$$U^\dagger t^a U = R^{ab}(U) t^b \tag{B3}$$

where $R^{ab}(U)$ defines the adjoint representation of the flavour group, we have that

$$j_5^{\mu,a}(x) \to R^{ab}(U) j_5^{\mu,b}(x), \tag{B4}$$

which is a flavour non-singlet quantity. In contrast, one may show following the same procedure that the current $j_5^{\mu,s}(x) = \bar\psi(x)\gamma_5\gamma^\mu\psi(x)$ is a flavour singlet.

Since gluons do not couple to flavour non-singlets, the diagram shown on Fig. 13. (*b*) is absent from the SDE of the non-singlet axial-vector vertex $t^a\Gamma_5^{\mu\nu}$, see Fig. 8. Instead, it must be added to the SDE of a singlet axial-vector vertex, see *e.g.*, [9].

Note that the non-singlet current is anomaly-free, see *e.g.*, [75], and thus is conserved in the chiral limit; in contrast,

the singlet current is not conserved in the same limit, displaying the Adler-Bell-Jackiw anomaly [143–147]. Specifically, the vertex $\Gamma_5^{\mu\nu\rho}(P,q,-r)$, Fig. 13. (*a*), which may be defined from the Fourier transform of the correlation function $\langle 0|T j_5^{\mu}(y)A^{\nu}(x_1)A^{\rho}(x_2)|0\rangle$, in complete analogy to Eq. (A.6), is transverse up the anomaly, that is

$$P_\mu \Gamma_5^{\mu\nu\rho}(P,q,-r) = 0 + \frac{ig^2}{16\pi^2} A^{\nu\rho}(P,q,-r), \tag{B5}$$

where the quantity $A^{\nu\rho}(P,q,-r)$ is defined from the Fourier transform of the anomalous term $\langle 0|T\epsilon^{\mu\sigma\kappa\delta}\mathrm{Tr}[F_{\kappa\delta}(x)F_{\mu\sigma}(x)]A^{\nu}(x_1)A^{\rho}(x_2)|0\rangle$, see, *e.g.*, [75].

References

1. C.D. Roberts, A.G. Williams, Prog. Part. Nucl. Phys. **33**, 477 (1994). https://doi.org/10.1016/0146-6410(94)90049-3
2. R. Alkofer, L. von Smekal, Phys. Rept. **353**, 281 (2001). https://doi.org/10.1016/S0370-1573(01)00010-2
3. P. Maris, C.D. Roberts, Int. J. Mod. Phys. E **12**, 297 (2003). https://doi.org/10.1142/S0218301303001326
4. C.S. Fischer, J. Phys. G **32**, R253 (2006). https://doi.org/10.1088/0954-3899/32/8/R02
5. C.D. Roberts, Prog. Part. Nucl. Phys. **61**, 50 (2008). https://doi.org/10.1016/j.ppnp.2007.12.034
6. D. Binosi, J. Papavassiliou, Phys. Rept. **479**, 1 (2009). https://doi.org/10.1016/j.physrep.2009.05.001
7. A. Maas, Phys. Rept. **524**, 203 (2013). https://doi.org/10.1016/j.physrep.2012.11.002
8. I.C. Cloet, C.D. Roberts, Prog. Part. Nucl. Phys. **77**, 1 (2014). https://doi.org/10.1016/j.ppnp.2014.02.001
9. G. Eichmann, H. Sanchis-Alepuz, R. Williams, R. Alkofer, C.S. Fischer, Prog. Part. Nucl. Phys. **91**, 1 (2016). https://doi.org/10.1016/j.ppnp.2016.07.001
10. C.S. Fischer, Prog. Part. Nucl. Phys. **105**, 1 (2019). https://doi.org/10.1016/j.ppnp.2019.01.002
11. M.Q. Huber, Phys. Rept. **879**, 1 (2020). https://doi.org/10.1016/j.physrep.2020.04.004
12. M.N. Ferreira, J. Papavassiliou, Particles **6**, 312 (2023). https://doi.org/10.3390/particles6010017
13. D. F. Litim and J. M. Pawlowski, in *Workshop on the Exact Renormalization Group* (1998) pp. 168–185
14. J. Berges, N. Tetradis, C. Wetterich, Phys. Rept. **363**, 223 (2002). https://doi.org/10.1016/S0370-1573(01)00098-9
15. J.M. Pawlowski, Annals Phys. **322**, 2831 (2007). https://doi.org/10.1016/j.aop.2007.01.007
16. B.-J. Schaefer, J. Wambach, Phys. Part. Nucl. **39**, 1025 (2008). https://doi.org/10.1134/S1063779608070083
17. H. Gies, Lect. Notes Phys. **852**, 287 (2012). https://doi.org/10.1007/978-3-642-27320-9_6
18. J. Braun, J. Phys. G **39**, 033001 (2012). https://doi.org/10.1088/0954-3899/39/3/033001
19. N. Dupuis, L. Canet, A. Eichhorn, W. Metzner, J.M. Pawlowski, M. Tissier, N. Wschebor, Phys. Rept. **910**, 1 (2021). https://doi.org/10.1016/j.physrep.2021.01.001
20. W.-J. Fu, Commun. Theor. Phys. **74**, 097304 (2022). https://doi.org/10.1088/1572-9494/ac86be
21. P. Maris, P.C. Tandy, Phys. Rev. C **60**, 055214 (1999). https://doi.org/10.1103/PhysRevC.60.055214
22. P. Maris, P.C. Tandy, Phys. Rev. C **61**, 045202 (2000). https://doi.org/10.1103/PhysRevC.61.045202
23. R. Alkofer, P. Watson, H. Weigel, Phys. Rev. D **65**, 094026 (2002). https://doi.org/10.1103/PhysRevD.65.094026
24. G. Eichmann, R. Alkofer, I.C. Cloet, A. Krassnigg, C.D. Roberts, Phys. Rev. C **77**, 042202 (2008). https://doi.org/10.1103/PhysRevC.77.042202
25. S.-X. Qin, L. Chang, Y.-X. Liu, C.D. Roberts, D.J. Wilson, Phys. Rev. C **84**, 042202 (2011). https://doi.org/10.1103/PhysRevC.84.042202
26. T. Hilger, C. Popovici, M. Gomez-Rocha, A. Krassnigg, Phys. Rev. D **91**, 034013 (2015). https://doi.org/10.1103/PhysRevD.91.034013
27. T. Hilger, M. Gomez-Rocha, A. Krassnigg, Phys. Rev. D **91**, 114004 (2015). https://doi.org/10.1103/PhysRevD.91.114004
28. B. El-Bennich, G. Krein, E. Rojas, F.E. Serna, Few Body Syst. **57**, 955 (2016). https://doi.org/10.1007/s00601-016-1133-x
29. F.F. Mojica, C.E. Vera, E. Rojas, B. El-Bennich, Phys. Rev. D **96**, 014012 (2017). https://doi.org/10.1103/PhysRevD.96.014012
30. K. Raya, M.A. Bedolla, J.J. Cobos-Martínez, A. Bashir, Few Body Syst. **59**, 133 (2018). https://doi.org/10.1007/s00601-018-1455-y
31. E. Weil, G. Eichmann, C.S. Fischer, R. Williams, Phys. Rev. D **96**, 014021 (2017). https://doi.org/10.1103/PhysRevD.96.014021
32. F.E. Serna, B. El-Bennich, G. Krein, Phys. Rev. D **96**, 014013 (2017). https://doi.org/10.1103/PhysRevD.96.014013
33. R.J. Hernández-Pinto, L.X. Gutiérrez-Guerrero, A. Bashir, M.A. Bedolla, I.M. Higuera-Angulo, Phys. Rev. D **107**, 054002 (2023). https://doi.org/10.1103/PhysRevD.107.054002
34. R.J. Hernández-Pinto, L.X. Gutiérrez-Guerrero, M.A. Bedolla, A. Bashir, Phys. Rev. D **110**, 114015 (2024). https://doi.org/10.1103/PhysRevD.110.114015
35. H. Munczek, Phys. Rev. D **52**, 4736 (1995). https://doi.org/10.1103/PhysRevD.52.4736
36. H.H. Matevosyan, A.W. Thomas, P.C. Tandy, Phys. Rev. C **75**, 045201 (2007). https://doi.org/10.1103/PhysRevC.75.045201
37. C.S. Fischer, D. Nickel, J. Wambach, Phys. Rev. D **76**, 094009 (2007). https://doi.org/10.1103/PhysRevD.76.094009
38. C.S. Fischer, R. Williams, Phys. Rev. D **78**, 074006 (2008). https://doi.org/10.1103/PhysRevD.78.074006
39. R. Williams, Eur. Phys. J. A **51**, 57 (2015). https://doi.org/10.1140/epja/i2015-15057-4
40. H. Sanchis-Alepuz, C.S. Fischer, S. Kubrak, Phys. Lett. B **733**, 151 (2014). https://doi.org/10.1016/j.physletb.2014.04.031
41. R. Williams, C.S. Fischer, W. Heupel, Phys. Rev. D **93**, 034026 (2016). https://doi.org/10.1103/PhysRevD.93.034026
42. H. Sanchis-Alepuz, R. Williams, Phys. Lett. B **749**, 592 (2015). https://doi.org/10.1016/j.physletb.2015.08.067
43. D. Binosi, L. Chang, J. Papavassiliou, S.-X. Qin, C.D. Roberts, Phys. Rev. D **93**, 096010 (2016). https://doi.org/10.1103/PhysRevD.93.096010
44. R. Williams, Phys. Lett. B **798**, 134943 (2019). https://doi.org/10.1016/j.physletb.2019.134943
45. Á. S. Miramontes, H. Sanchis Alepuz, and R. Alkofer, Phys. Rev. D **103**, 116006 (2021)https://doi.org/10.1103/PhysRevD.103.116006
46. Á.S. Miramontes, R. Alkofer, C.S. Fischer, H. Sanchis-Alepuz, Phys. Lett. B **833**, 137291 (2022). https://doi.org/10.1016/j.physletb.2022.137291
47. F. Gao, A.S. Miramontes, J. Papavassiliou, J.M. Pawlowski, Phys. Lett. B **863**, 139384 (2025). https://doi.org/10.1016/j.physletb.2025.139384
48. A.S. Miramontes, G. Eichmann, R. Alkofer, Phys. Lett. B **868**, 139659 (2025). https://doi.org/10.1016/j.physletb.2025.139659
49. W.-j. Fu, C. Huang, J. M. Pawlowski, Y.-y. Tan, and L.-j. Zhou, (2025), arXiv: 2502.14388 [hep-ph]
50. M. Chen, L. Chang, Chin. Phys. C **43**, 114103 (2019). https://doi.org/10.1088/1674-1137/43/11/114103

51. L. Chang, M. Ding, Phys. Rev. D **103**, 074001 (2021). https://doi.org/10.1103/PhysRevD.103.074001
52. Y.-Z. Xu, JHEP **2024** (7), 118https://doi.org/10.1007/JHEP07(2024)118
53. Y.-Z. Xu, Phys. Rev. D **111**, 114012 (2025). https://doi.org/10.1103/399s-4jrq
54. Y.Z. Xu, K. Raya, J. Rodríguez-Quintero, J. Segovia, Phys. Rev. D **110**, 054031 (2024). https://doi.org/10.1103/PhysRevD.110.054031
55. A.C. Aguilar, D. Binosi, J. Papavassiliou, J. Rodriguez-Quintero, Phys. Rev. D **80**, 085018 (2009). https://doi.org/10.1103/PhysRevD.80.085018
56. D. Binosi, L. Chang, J. Papavassiliou, C.D. Roberts, Phys. Lett. B **742**, 183 (2015). https://doi.org/10.1016/j.physletb.2015.01.031
57. Z.-F. Cui, J.-L. Zhang, D. Binosi, F. Soto, C. Mezrag, J. Papavassiliou, C.D. Roberts, J. Rodríguez-Quintero, J. Segovia, S. Zafeiropoulos, Chin. Phys. C **44**, 083102 (2020). https://doi.org/10.1088/1674-1137/44/8/083102
58. A. Deur, S.J. Brodsky, C.D. Roberts, Prog. Part. Nucl. Phys. **134**, 104081 (2024). https://doi.org/10.1016/j.ppnp.2023.104081
59. P. Maris and C. D. Roberts, https://doi.org/10.1103/PhysRevC.56.3369 Phys. Rev. C **56**, 3369 (1997)
60. H. Sanchis-Alepuz, R. Williams, J. Phys: Conf. Ser. **631**, 012064 (2015). https://doi.org/10.1088/1742-6596/631/1/012064
61. D. Nicmorus, G. Eichmann, A. Krassnigg, R. Alkofer, Phys. Rev. D **80**, 054028 (2009). https://doi.org/10.1103/PhysRevD.80.054028
62. G. Eichmann, R. Alkofer, A. Krassnigg, D. Nicmorus, Phys. Rev. Lett. **104**, 201601 (2010). https://doi.org/10.1103/PhysRevLett.104.201601
63. G. Eichmann, Phys. Rev. D **84**, 014014 (2011). https://doi.org/10.1103/PhysRevD.84.014014
64. W. Heupel, G. Eichmann, C.S. Fischer, Phys. Lett. B **718**, 545 (2012). https://doi.org/10.1016/j.physletb.2012.11.009
65. H. Sanchis-Alepuz, G. Eichmann, S. Villalba-Chavez, R. Alkofer, Phys. Rev. D **84**, 096003 (2011). https://doi.org/10.1103/PhysRevD.84.096003
66. H. Sanchis-Alepuz, R. Williams, R. Alkofer, Phys. Rev. D **87**, 096015 (2013). https://doi.org/10.1103/PhysRevD.87.096015
67. P.C. Wallbott, G. Eichmann, C.S. Fischer, Phys. Rev. D **100**, 014033 (2019). https://doi.org/10.1103/PhysRevD.100.014033
68. Z.Q. Yao, Y.Z. Xu, D. Binosi, Z.F. Cui, M. Ding, K. Raya, C.D. Roberts, J. Rodríguez-Quintero, S.M. Schmidt, Eur. Phys. J. A **61**, 92 (2025). https://doi.org/10.1140/epja/s10050-025-01557-x
69. G. Eichmann, R.D. Torres, Phys. Rev. D **111**, 094008 (2025). https://doi.org/10.1103/PhysRevD.111.094008
70. G. Eichmann, M.T. Peña, R.D. Torres, Phys. Lett. B **866**, 139525 (2025). https://doi.org/10.1016/j.physletb.2025.139525
71. J.C. Ward, Phys. Rev. **78**, 182 (1950). https://doi.org/10.1103/PhysRev.78.182
72. Y. Takahashi, Nuovo Cim. **6**, 371 (1957). https://doi.org/10.1007/BF02832514
73. K. Fujikawa, Phys. Rev. D **21**, 2848 (1980). https://doi.org/10.1103/PhysRevD.21.2848. (**[Erratum: Phys. Rev. D 22, 1499 (1980)]**)
74. C. Itzykson and J. B. Zuber, *Quantum Field Theory*, International Series in Pure and Applied Physics (New York, USA: Mcgraw-Hill (1980) 705 p., 1980)
75. V. A. Miransky, *Dynamical symmetry breaking in quantum field theories* (World Scientific, 1994) https://doi.org/10.1142/2170
76. H. Gies, C. Wetterich, Phys. Rev. D **69**, 025001 (2004). https://doi.org/10.1103/PhysRevD.69.025001
77. J.M. Pawlowski, D.F. Litim, S. Nedelko, L. Smekal, Phys. Rev. Lett. **93**, 152002 (2004). https://doi.org/10.1103/PhysRevLett.93.152002
78. C. S. Fischer and H. Gies, JHEP **10**, 048https://doi.org/10.1088/1126-6708/2004/10/048
79. F.J. Llanes-Estrada, C.S. Fischer, R. Alkofer, Nucl. Phys. Proc. Suppl. **152**, 43 (2006). https://doi.org/10.1016/j.nuclphysbps.2005.08.008
80. R. Alkofer, C.S. Fischer, F.J. Llanes-Estrada, K. Schwenzer, Annals Phys. **324**, 106 (2009). https://doi.org/10.1016/j.aop.2008.07.001
81. A. Windisch, M. Hopfer, R. Alkofer, Acta Phys. Polon. Supp. **6**, 347 (2013). https://doi.org/10.5506/APhysPolBSupp.6.347
82. M. Hopfer, A. Windisch, and R. Alkofer, PoS **ConfinementX**, 073 (2012)https://doi.org/10.22323/1.171.0073
83. M. Mitter, J.M. Pawlowski, N. Strodthoff, Phys. Rev. D **91**, 054035 (2015). https://doi.org/10.1103/PhysRevD.91.054035
84. A.C. Aguilar, D. Binosi, D. Ibañez, J. Papavassiliou, Phys. Rev. D **90**, 065027 (2014). https://doi.org/10.1103/PhysRevD.90.065027
85. J. Braun, L. Fister, J.M. Pawlowski, F. Rennecke, Phys. Rev. D **94**, 034016 (2016). https://doi.org/10.1103/PhysRevD.94.034016
86. F. Rennecke, Phys. Rev. D **92**, 076012 (2015). https://doi.org/10.1103/PhysRevD.92.076012
87. A.C. Aguilar, J.C. Cardona, M.N. Ferreira, J. Papavassiliou, Phys. Rev. D **96**, 014029 (2017). https://doi.org/10.1103/PhysRevD.96.014029
88. A.K. Cyrol, M. Mitter, J.M. Pawlowski, N. Strodthoff, Phys. Rev. D **97**, 054006 (2018). https://doi.org/10.1103/PhysRevD.97.054006
89. A.C. Aguilar, J.C. Cardona, M.N. Ferreira, J. Papavassiliou, Phys. Rev. D **98**, 014002 (2018). https://doi.org/10.1103/PhysRevD.98.014002
90. O. Oliveira, T. Frederico, W. de Paula, J.P.B.C. de Melo, Eur. Phys. J. C **78**, 553 (2018). https://doi.org/10.1140/epjc/s10052-018-6037-0
91. O. Oliveira, W. de Paula, T. Frederico, J.P.B.C. de Melo, Eur. Phys. J. C **79**, 116 (2019). https://doi.org/10.1140/epjc/s10052-019-6617-7
92. L. Albino, A. Bashir, L.X.G. Guerrero, B.E. Bennich, E. Rojas, Phys. Rev. D **100**, 054028 (2019). https://doi.org/10.1103/PhysRevD.100.054028
93. W.-J. Fu, J.M. Pawlowski, F. Rennecke, Phys. Rev. D **101**, 054032 (2020). https://doi.org/10.1103/PhysRevD.101.054032
94. C. Tang, F. Gao, Y.-X. Liu, Phys. Rev. D **100**, 056001 (2019). https://doi.org/10.1103/PhysRevD.100.056001
95. M.Q. Huber, Phys. Rev. D **101**, 114009 (2020). https://doi.org/10.1103/PhysRevD.101.114009
96. O. Oliveira, T. Frederico, W. de Paula, Eur. Phys. J. C **80**, 484 (2020). https://doi.org/10.1140/epjc/s10052-020-8037-0
97. F. Gao, J. Papavassiliou, J.M. Pawlowski, Phys. Rev. D **103**, 094013 (2021). https://doi.org/10.1103/PhysRevD.103.094013
98. L. Albino, A. Bashir, B. El-Bennich, E. Rojas, F. E. Serna, and R. C. da Silveira, JHEP **2021** (11), 196https://doi.org/10.1007/JHEP11(2021)196
99. A.C. Aguilar, M.N. Ferreira, B.M. Oliveira, J. Papavassiliou, G.T. Linhares, Eur. Phys. J. C **84**, 1231 (2024). https://doi.org/10.1140/epjc/s10052-024-13605-9
100. J. Skullerud and A. Kizilersu, J. High Energy Phys. **2002** (09), 013https://doi.org/10.1088/1126-6708/2002/09/013
101. J. I. Skullerud, P. O. Bowman, A. Kizilersu, D. B. Leinweber, and A. G. Williams, J. High Energy Phys. **2003** (04), 047https://doi.org/10.1088/1126-6708/2003/04/047
102. J.I. Skullerud, P.O. Bowman, A. Kizilersu, D.B. Leinweber, A.G. Williams, Nucl. Phys. Proc. Suppl. **141**, 244 (2005). https://doi.org/10.1016/j.nuclphysbps.2004.12.037
103. E.-M. Ilgenfritz, M. Muller-Preussker, A. Sternbeck, A. Schiller, I. Bogolubsky, Braz. J. Phys. **37**, 193 (2007). https://doi.org/10.1590/S0103-97332007000200006

104. A. Kizilersu, D.B. Leinweber, J.-I. Skullerud, A.G. Williams, Eur. Phys. J. C **50**, 871 (2007). https://doi.org/10.1140/epjc/s10052-007-0250-6
105. I. Bogolubsky, E. Ilgenfritz, M. Muller-Preussker, and A. Sternbeck, PoS **LATTICE2007**, 290 (2007) https://doi.org/10.22323/1.042.0290
106. I. Bogolubsky, E. Ilgenfritz, M. Muller-Preussker, A. Sternbeck, Phys. Lett. B **676**, 69 (2009). https://doi.org/10.1016/j.physletb.2009.04.076
107. O. Oliveira and P. Silva, PoS **LAT2009**, 226 (2009)https://doi.org/10.22323/1.091.0226
108. O. Oliveira, P. Bicudo, J. Phys. G **G38**, 045003 (2011). https://doi.org/10.1088/0954-3899/38/4/045003
109. A. Ayala, A. Bashir, D. Binosi, M. Cristoforetti, J. Rodriguez-Quintero, Phys. Rev. D **86**, 074512 (2012). https://doi.org/10.1103/PhysRevD.86.074512
110. A. Sternbeck, M. Müller-Preussker, Phys. Lett. B **726**, 396 (2013). https://doi.org/10.1016/j.physletb.2013.08.017
111. P. Bicudo, D. Binosi, N. Cardoso, O. Oliveira, P.J. Silva, Phys. Rev. D **92**, 114514 (2015). https://doi.org/10.1103/PhysRevD.92.114514
112. A.G. Duarte, O. Oliveira, P.J. Silva, Phys. Rev. D **94**, 014502 (2016). https://doi.org/10.1103/PhysRevD.94.014502
113. A. Sternbeck, P.-H. Balduf, A. Kizilersu, O. Oliveira, P. J. Silva, J.-I. Skullerud, and A. G. Williams, PoS **LATTICE2016**, 349 (2017)https://doi.org/10.22323/1.256.0349
114. P. Boucaud, F. Soto, J. Rodríguez-Quintero, S. Zafeiropoulos, Phys. Rev. D **95**, 114503 (2017). https://doi.org/10.1103/PhysRevD.95.114503
115. A.C. Aguilar, F. De Soto, M.N. Ferreira, J. Papavassiliou, J. Rodríguez-Quintero, S. Zafeiropoulos, Eur. Phys. J. C **80**, 154 (2020). https://doi.org/10.1140/epjc/s10052-020-7741-0
116. A.C. Aguilar, F. Soto, M.N. Ferreira, J. Papavassiliou, J. Rodríguez-Quintero, Phys. Lett. B **818**, 136352 (2021). https://doi.org/10.1016/j.physletb.2021.136352
117. A. Kızılersü, O. Oliveira, P.J. Silva, J.-I. Skullerud, A. Sternbeck, Phys. Rev. D **103**, 114515 (2021). https://doi.org/10.1103/PhysRevD.103.114515
118. J.-I. Skullerud, A. Kızılersü, O. Oliveira, P. Silva, and A. Sternbeck, PoS **LATTICE2021**, 305 (2022)https://doi.org/10.22323/1.396.0305
119. L. Chang, Y.-B. Liu, K. Raya, J. Rodríguez-Quintero, Y.-B. Yang, Phys. Rev. D **104**, 094509 (2021). https://doi.org/10.1103/PhysRevD.104.094509
120. F. Pinto-Gómez, F. Soto, M.N. Ferreira, J. Papavassiliou, J. Rodríguez-Quintero, Phys. Lett. B **838**, 137737 (2023). https://doi.org/10.1016/j.physletb.2023.137737
121. F. Pinto-Gómez, F. Soto, J. Rodríguez-Quintero, Phys. Rev. D **110**, 014005 (2024). https://doi.org/10.1103/PhysRevD.110.014005
122. A. Bender, W. Detmold, C. Roberts, A.W. Thomas, Phys. Rev. C **65**, 065203 (2002). https://doi.org/10.1103/PhysRevC.65.065203
123. M. Bhagwat, A. Holl, A. Krassnigg, C. Roberts, P. Tandy, Phys. Rev. C **70**, 035205 (2004). https://doi.org/10.1103/PhysRevC.70.035205
124. L. Chang, C.D. Roberts, Phys. Rev. Lett. **103**, 081601 (2009). https://doi.org/10.1103/PhysRevLett.103.081601
125. K. Fujikawa, B.W. Lee, A.I. Sanda, Phys. Rev. D **6**, 2923 (1972)
126. A. Kizilersu, M. Reenders, M. Pennington, Phys. Rev. D **52**, 1242 (1995). https://doi.org/10.1103/PhysRevD.52.1242
127. A.I. Davydychev, P. Osland, L. Saks, Phys. Rev. D **63**, 014022 (2001). https://doi.org/10.1103/PhysRevD.63.014022
128. D. Binosi, L. Chang, J. Papavassiliou, S.-X. Qin, C.D. Roberts, Phys. Rev. D **95**, 031501 (2017). https://doi.org/10.1103/PhysRevD.95.031501
129. J. Berges, Phys. Rev. D **70**, 105010 (2004). https://doi.org/10.1103/PhysRevD.70.105010
130. J. Berges, A.I.P. Conf, Proc. **739**, 3 (2004). https://doi.org/10.1063/1.1843591
131. M. C. A. York, G. D. Moore, and M. Tassler, JHEP **2021** (06), 077 https://doi.org/10.1007/JHEP06(2012)077
132. M.E. Carrington, Y. Guo, Phys. Rev. D **83**, 016006 (2011). https://doi.org/10.1103/PhysRevD.83.016006
133. P. Maris, C.D. Roberts, P.C. Tandy, Phys. Lett. B **420**, 267 (1998). https://doi.org/10.1016/S0370-2693(97)01535-9
134. A.C. Aguilar, D. Ibañez, J. Papavassiliou, Phys. Rev. D **87**, 114020 (2013). https://doi.org/10.1103/PhysRevD.87.114020
135. M.N. Ferreira, J. Papavassiliou, Prog. Part. Nucl. Phys. **144**, 104186 (2025). https://doi.org/10.1016/j.ppnp.2025.104186
136. A. Salam, Phys. Rev. **130**, 1287 (1963). https://doi.org/10.1103/PhysRev.130.1287
137. A. Salam, R. Delbourgo, Phys. Rev. **135**, B1398 (1964). https://doi.org/10.1103/PhysRev.135.B1398
138. R. Delbourgo, P.C. West, J. Phys. A **10**, 1049 (1977). https://doi.org/10.1088/0305-4470/10/6/024
139. R. Delbourgo, P.C. West, Phys. Lett. B **72**, 96 (1977). https://doi.org/10.1016/0370-2693(77)90071-5
140. L.F. Abbott, P. Sikivie, M.B. Wise, Phys. Rev. D **21**, 1393 (1980). https://doi.org/10.1103/PhysRevD.21.1393
141. J.S. Ball, T.-W. Chiu, Phys. Rev. D **22**, 2542 (1980). https://doi.org/10.1103/PhysRevD.22.2542
142. D. Binosi and J. Papavassiliou, J. High Energy Phys. **03**, 121https://doi.org/10.1007/JHEP03(2011)121
143. J.S. Schwinger, Phys. Rev. **82**, 664 (1951). https://doi.org/10.1103/PhysRev.82.664
144. J.S. Schwinger, Phys. Rev. **128**, 2425 (1962). https://doi.org/10.1103/PhysRev.128.2425
145. S.L. Adler, Phys. Rev. **177**, 2426 (1969). https://doi.org/10.1103/PhysRev.177.2426
146. J.S. Bell, R. Jackiw, Nuovo Cim. A **60**, 47 (1969). https://doi.org/10.1007/BF02823296
147. W.A. Bardeen, Phys. Rev. **184**, 1848 (1969). https://doi.org/10.1103/PhysRev.184.1848